Final Report

Assessment of Dispersant Effectiveness Using Ultrasound to Measure Oil Droplet Particle Size Distributions

For

U.S. Department of the Interior
Bureau of Safety and Environmental Enforcement (BSEE)
Herndon, VA

Project # 697

Submitted By

Paul D. Panetta[1,2], Leslie G. Bland[1,*], Kyle Winfield[1], and Dale McElhone[1,2]

And

Grace G. Cartwright[2] and Carl T. Friedrichs[2]

[1]Applied Research Associates, Inc.

[2]The College of William & Mary, Virginia Institute of Marine Science

[*]Now at the University of Virginia

February 2013

Study concept, oversight, and funding were provided by the U.S. Department of the Interior, Bureau of Safety and Environmental Enforcement, Washington, DC under Contract Number E12PC00011.

ACKNOWLEDGMENTS

The authors wish to thank Wayne Reisner from the Virginia Institute of Marine Science for fabricating the sample chambers, Tim Nedwed from ExxonMobil for inviting us during their dispersant testing at Ohmsett, Randy Belore from S.L.Ross, Al Guarino from Mar, Inc. for assistance at Ohmsett and Per Johan Brandvik and the Sintef team for access to the Sintef Tower Basin and assistance during testing at Sintef.

DISCLAIMER

TABLE OF CONTENTS

EXECUTIVE SUMMARY

During the Deepwater Horizon incident, 1.84 million gallons of chemical dispersants were used, including 771,000 gallons at the wellhead [Deepwater Report to the President]. The main effect of dispersants on oil is to decrease the droplet size of the oil to a size that will remain within the interior of the water column by natural motion, long enough to be consumed by naturally occurring bacteria [Lewis and Aurand]. At that time, the state-of-the-art in monitoring the effectiveness of dispersants was to collect oil samples near the blowout and bring them back to a laboratory for analysis. A second method was to observe the size of the surface slick after the dispersant was applied at the wellhead to see if the slick decreased in size. These methods are indirect and not timely – the development of in-situ techniques offers considerable promise for improvement.

In this project, we developed acoustic techniques to measure dispersed oil droplet size in-situ to enable future monitoring at the high concentrations experienced during oil well blowouts. We demonstrated the proof-of-concept through numerous tests in the lab and two trips to Ohmsett for measurements on surface slicks. The Ohmsett data were collected in conjunction with ExxonMobil dispersant testing over 6 days, with one day in December 2011 and five days in August 2012. In addition, we were able to piggy-back on subsurface oil release experiments at the Sintef Tower Basin tank, which was not originally part of the scope of the project. The Sintef experiments helped us to understand the differences between surface slicks and subsurface releases.

Acoustics have been used in ocean environments for many decades for imaging and identifying various objects (fish, submarines, etc.) and for mapping the bathymetry of the seafloor. However, sonar instruments are tuned to image targets rather than provide physical parameters over small scales such as the size of oil droplets, which can be on the order of 10s to 100s of microns. We advanced the state-of-the-art beyond sonar imaging to quantitatively measure the oil droplet size using acoustic frequencies between 0.5 MHz and 5 MHz.

The measurements performed at Sintef showed subsurface releases of oil and applications of dispersants create different measurement challenges relative to above-water dispersant applications to surface slicks. More specifically, the oil concentration is higher in a subsurface blowout, the oil is more localized near the blowout rather than spread out, and the droplet speeds are dramatically different between surface slicks (low speed) and blowouts (high speed). Additional testing is needed on subsurface releases to further develop these methods.

In addition to the testing with precision acoustic equipment, we assessed commercial sonar and a marine acoustic instrument for future technology transfer of our methods. These instruments included a rotary sonar system manufactured by Imagenex operating between 320 kHz and 1 MHz and an Acoustic Doppler Velocimeter (ADV) manufactured by Sontek, which operates at 5 MHz. Based on our findings we

believe that both instruments have the potential for immediate application and future technology transfer. The rotary sonar system has more immediate applicability because of the large frequency range it spans.

The oil spill response community needs to know many parameters in order to optimize applications of dispersants to subsea blowouts. Parameters of interest include the size distribution of the oil droplets, the presence and size distribution of gas hydrates and gas bubbles, the presence and size distribution of any sediment, and the dynamics of these constituents as a function of depth, temperature, salinity, and dispersant-to-oil ratio (DOR) [Ahnell, Nedwed]. Our focus in this project was to take the first step toward developing a suite of measurement tools addressing these needs. We successfully developed acoustic methods to measure dispersed oil droplet size that were presented at several conferences including Clean Pacific, Clean Gulf, Oceans 12, and an American Petroleum Institute (API) oil fate and transport modeling workshop.

We recommend a “two-pronged” approach for future development; one path should focus on instrument development and a second path on scientific studies. The goal of the first path will be to develop acoustic instruments at specific frequencies to optimally excite droplets so that the instruments can measure the transition from large droplets that will rise to the surface to small droplets that will stay entrained in the water column after a dispersant application. The goal of the second path will be to continue the scientific study of multi-particulate plumes to develop methods to accurately measure key parameters in-situ (as listed above) to help optimize the application of dispersant to subsea blowout oil.

1. OBJECTIVE

The objective of this project was to develop acoustic methods and technologies to determine the effectiveness of dispersants by directly measuring the change of oil droplet size. Developing the tools to measure oil droplet size in-situ will improve spill response by providing the location and amount of the dispersed oil and enable optimum application of dispersants to the affected area. In addition, these tools will improve the inputs to models used to predict the fate and transport of oil.

2. OVERVIEW

Dispersants play an important role in oil spill response by decreasing the spread and impact from surface oil spills and subsea blowouts. Subsea dispersant used during the Deepwater Horizon incident (also known as the Macondo blowout) introduced the spill response community to dispersant injection directly into a flowing plume of oil and natural gas over 1500 meters below the ocean surface. While the application of 1.84 million gallons of dispersant during the incident was intended to help the oil to naturally biodegrade by keeping oil from rising to the surface, there were no measurement tools to determine dispersant efficacy in-situ.

Figure 1 shows dispersant applications to the Macondo blowout using three different configurations - a single nozzle, three nozzles, and a ring with multiple outlets. The dispersant is the white fluid moving toward the brown oil plume. Dispersants are designed to keep the oil in suspension by decreasing the droplet size enough to overcome the buoyant force through natural turbulence in the water column. This decrease in size is accomplished by decreasing the surface tension at the oil-water interface, causing the oil to form smaller droplets. When the droplet size decreases to less than ~70 microns in diameter, the droplets remain suspended within the interior of the water column long enough to be consumed by naturally occurring bacteria [Lewis and Aurand].

Currently, the efficacy of dispersants applied aerially to surface oil slicks is monitored by measuring the droplet size decrease using a Laser In-Situ Scattering Transmissometer (LISST) or the concentration of oil in the water column using fluorometers. Figure 2 shows a typical droplet size distribution of crude oil and a crude oil-dispersant mixture measured with a LISST during our experiments. However, applicability of commercial LISST instruments is limited to dilute mixtures, below ~500 ppm. In addition, the LISST cannot distinguish oil droplets from gas bubbles, and the sensor windows quickly become occluded by oil and biofilms. In our testing, the

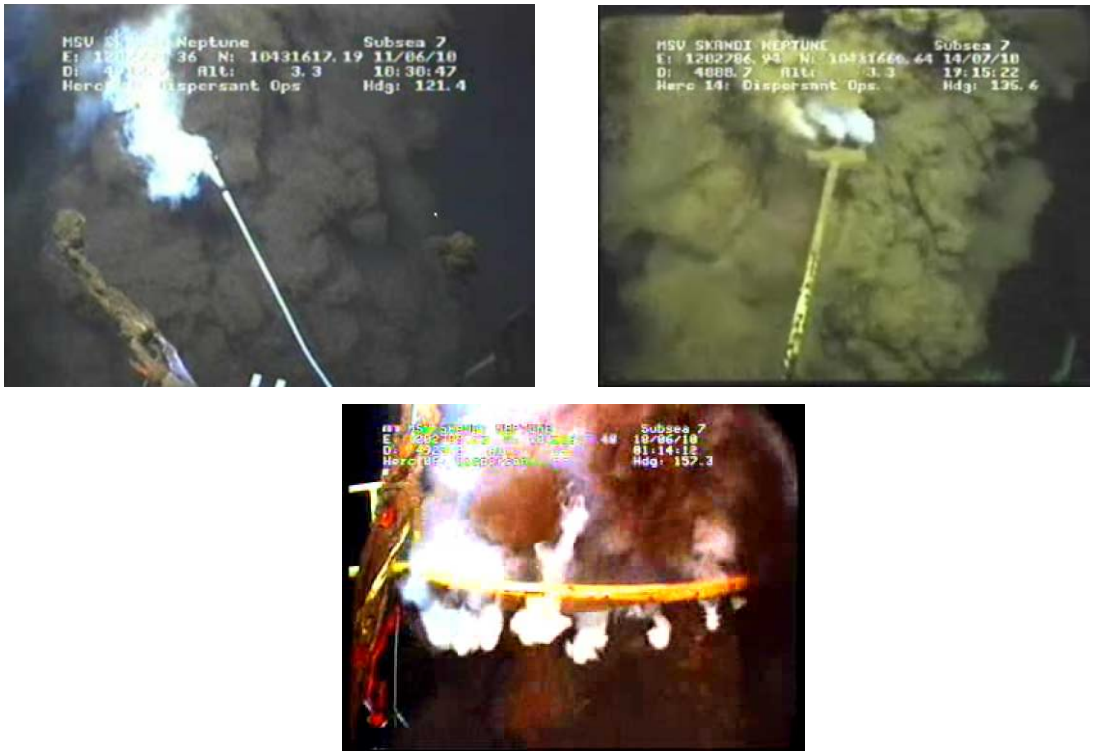

Figure 1. Photographs of dispersant being applied to the Deepwater Horizon plume using three different methods. The dispersant is the white fluid being sprayed onto the brown oil.

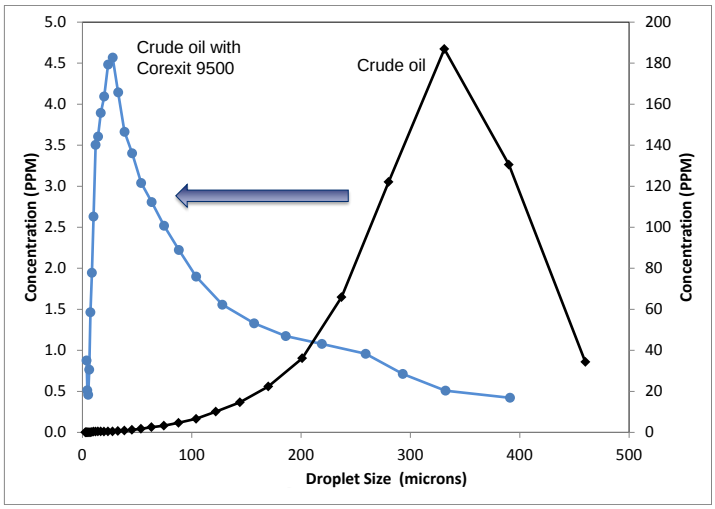

Figure 2. Droplet size distribution determined by LISST for crude oil and crude oil mixed with the commercial dispersant Corexit 9500 in a laboratory experiment.

windows needed to be cleaned several times per day, while the response of the acoustic sensors was not affected by oil films. Furthermore, fluorometers only measure oil concentration; thus, they cannot distinguish between naturally dispersed oil, which will float back to the surface, from chemically dispersed oil droplets [Nedwed]. Clearly, there is a need for instrumentation that can directly measure the droplet size in a concentrated oil plume (e.g., subsea oil well blowout).

The Applied Research Associates, Inc. (ARA) team embarked on this project to develop acoustic methods to measure oil droplet size in-situ. We conducted experiments in the lab, during two field trips to Ohmsett, in a large wave tank operated by Mar Inc. for the Department of Interior, and at Sintef's Tower Basin tank (a 3 meter wide by 6 meter deep tank used to simulate subsurface releases). Details of these experiments are discussed in subsequent sections of this report. We presented the results of our work at several conferences and workshops including Clean Pacific, Clean Gulf, Oceans 12 and an API workshop on oil fate and transport. The results presented at the Oceans 12 conference were published in the conference proceedings [Panetta et al. 2012]. These conferences provided useful feedback and peer review from members of the oil spill response and scientific communities. In the sections that follow, we present the experimental results, conclusions, and recommendations for future work.

3. TECHNICAL METHODS AND RESULTS

To develop acoustic methods to measure oil droplet size we executed four tasks. First, we performed measurements in our laboratory to determine the optimum acoustic frequency range and best measurement methods. We followed these laboratory experiments with field experiments at Ohmsett and Sintef. In the third and fourth tasks,

we performed theoretical calculations to model the acoustic scattering and resonances of oil droplets and developed algorithms to calculate the oil droplet size from the acoustic scattering data.

In the first task, we performed measurements on 6 crude oils with two dispersants as shown in Table 1. The gel dispersant is a new formulation developed by ExxonMobil and is not yet available commercially. We also chose to experiment with Corexit 9500 because it was the most widely used dispersant applied to the Deep Horizon blowout and is currently the most commonly employed dispersant. The gel dispersant was selected because its rheological properties were very different than Corexit. We originally planned to use Agma DR 379, but since it is not approved for use in the US, we chose not to study it.

Table 1. Crude oil and dispersant combinations used in this study (indicated by check marks).

Oil	Corexit 9500	Gel Dispersant
Dorado	✓	
Endicott - Fresh	✓	
Endicott Emulsion	✓	✓
Hebron	✓	✓
Sockeye Emulsion	✓	✓
Venoco Emulsion	✓	✓

3.1 Acoustic Theory

When an acoustic wave traverses dispersed oil, the waves scatter at the droplet-fluid interface due to a mismatch of the acoustic properties at the boundary caused by the density and viscosity differences between the oil and water. The droplets also oscillate back and forth in the traveling wave, and can change shape through resonant vibrations. The scattered signals create the reflections we see in sonar images, fish finders, and medical ultrasound images. In addition to providing an imaging modality, the scattering removes energy from the acoustic field, causing it to attenuate as it propagates through the dispersion. The droplet motion and the shape changes also remove energy from the acoustic field, further decreasing the acoustic field amplitude. In compressible particles, like gas bubbles, energy is efficiently absorbed and reradiated when the acoustic frequency matches the resonant frequency of the particle. This absorption and reradiation can be measured as backscattering and forward-going attenuation. Each of these mechanisms is related to the droplet size and chemical properties. Therefore, by carefully measuring the acoustic field and understanding these interactions, one can determine the sizes of the oil droplets and/or gas bubbles. Schematic representations of these mechanisms for an oil-water mixture are shown in Figure 3. In this figure, the sound field is propagating from the left and impinging on the droplets. The sound scatters in all directions as shown by the light blue arrows. The droplet motion and shape change are shown in the two right-hand schematics independent of the scattered field.

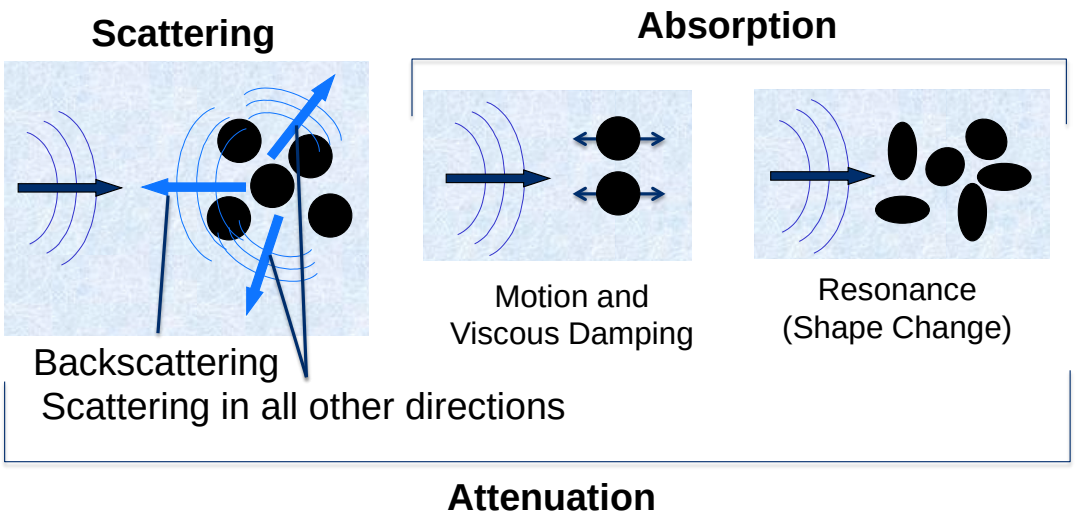

Figure 3. Schematic of scattering and absorption mechanisms for an acoustic field traveling through oil droplets in water. The black circles represent the oil droplets. The acoustic wave is represented by curved wave fronts moving in the direction of the arrows.

Many aspects of the acoustic field can be used to measure the properties of oil droplets, including the speed of sound, the attenuation, and the backscattering. We focused on the backscattered field, which returns directly back to the transmitting transducer, because of its simplicity for deployment and the wealth of information that can be obtained from it. The backscattering measurement is especially appealing because it eliminates alignment inaccuracies that can be associated with methods that use multiple transducers. In addition, the backscattering can be used to determine attenuation, adding a second parameter that can be measured from a single transducer [Panetta et al. 2002, Panetta et al. 2003, Panetta 2010].

The resonant frequency of a gas bubble or oil droplet is given by [Urick]

$$f_r = \frac{1}{2\pi a}\sqrt{\frac{3\gamma P}{\rho}}$$

where

a = radius of the bubble or droplet
γ = ratio of specific heats of the gas bubble or oil droplet
P = hydrostatic pressure
ρ = density of the water

For liquid oil with γ =1, at zero depth in the sea with P= 1 atmosphere

$$f_r = \frac{276}{a}$$

For a 100 micron diameter oil droplet in water at sea level, the resonant frequency is 55 kHz.

The scattering from an elastic fluid sphere is given by [Medwin]

$$\sigma_s(f) = 4\pi a^2 (ka)^4 \left[\left(\frac{e-1}{3e} \right)^2 + \frac{1}{3} \left(\frac{g-1}{2g+1} \right)^2 \right]$$

where
f = acoustic frequency
a = radius of the sphere
k = 2πf/v, with v = the speed of sound in the surrounding medium
e = ratio of bulk modulus of sphere to that of surrounding medium
g = ratio of density of sphere to that in the surrounding medium

The scattering per steradian provides the following equation for backscattering

$$\sigma_{bs}(f) = a^2 (ka)^4 \left[\left(\frac{e-1}{3e} \right)^2 + \frac{1}{3} \left(\frac{g-1}{2g+1} \right)^2 \right]$$

The total backscattering S is calculated from the equation below where the backscattering cross section, σ_{bs}, is integrated over the droplet size distribution, given by n(a).

$$S = \int \sigma_{bs}(a)\, n(a)\, da$$

Particular distributions observed by the LISST during our testing at Ohmsett in 2012 for Run 9 and Run 12 are shown in Figure 4. The details of these experiments will be described in subsequent sections. The average droplet size from these runs is ~9 microns and ~ 65 microns, respectively. The integrand of the total backscatter equation above is shown in Figure 5 as a function of droplet radius for the droplet size distributions from Run 9 and Run 12. The radius-dependent total backscatter and

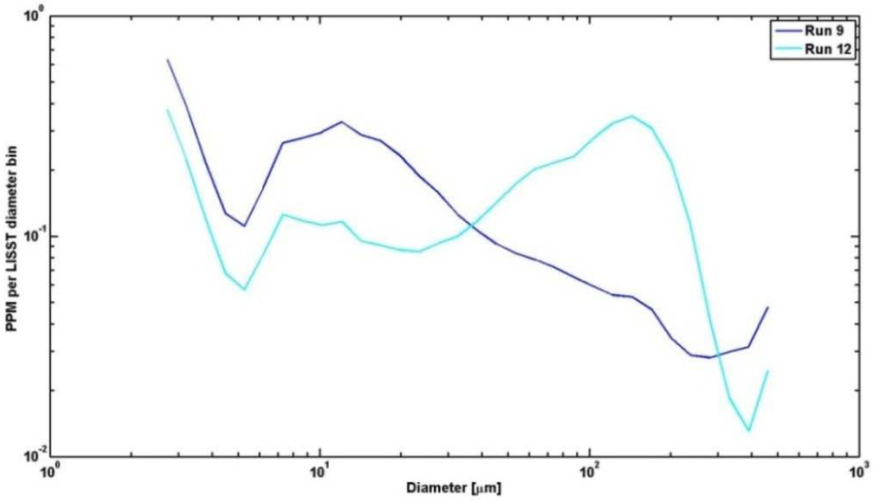

Figure 4. Oil droplet size distributions for Run 9 and Run 12 during testing at Ohmsett in August 2012.

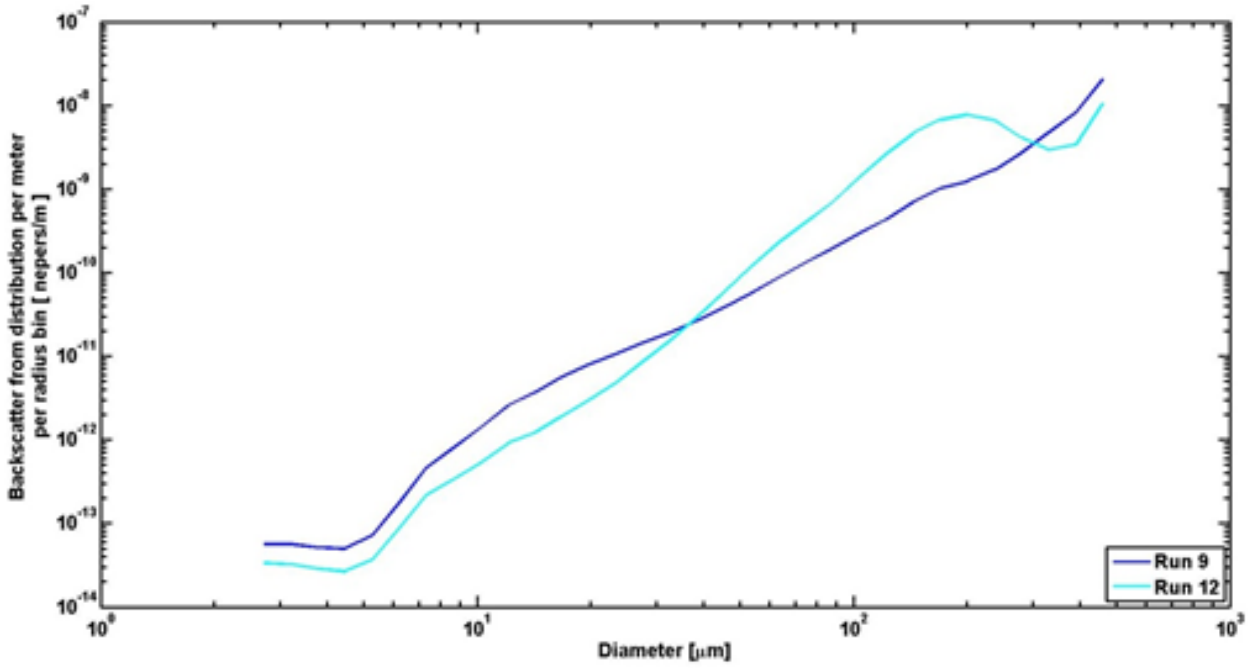

Figure 5. The backscatter vs. droplet diameter for a 1 MHz acoustic wave in Run 9 at Ohmsett.

extinction per meter for the distributions are calculated by multiplying the cross sections by the number densities for the two distributions.

For the measurements in August at 1 MHz, there were many small droplets with a diameter of ~6 microns and a corresponding resonant frequency at ~920 kHz, causing the wave propagation to be dominated by resonance rather than the scattering. Based on these theoretical findings and observations, we chose to work at 5 MHz to limit the resonance effects. Future work on oil-gas bubble mixtures will exploit these resonant effects to help separate the contributions to acoustic scattering and attenuation.

3.2 LABORATORY EXPERIMENTS

For our acoustic measurements we used a commercially available precision instrument from Peak NDT shown in Figure 6. It has a frequency range from 500 kHz to 25 MHz and a 16 bit digitizer with a sampling rate up to 200 MSamples/second. The system has two channels that can be pulsed independently in a monostatic configuration or in conjunction with one pulsing and another receiving in a bi-static configuration. This precision acoustic instrument is controlled by the Inspectionware software platform which allows complete customization of the data acquisition and analysis in one software tool. We are able to save the complete acoustic waveform, perform frequency analysis, customize the pulse voltage, signal average, change gain, employ time windowing, and perform multiple complex analysis routines. The system can also perform most imaging routines that commercial sonar instruments use with the

added benefit that we can capture and store the complete acoustic signal for immediate or later processing.

To benchmark the acoustic measurements, the droplet size distribution was measured directly using a LISST-100X instrument manufactured by Sequoia Scientific Inc. The LISST uses laser diffraction to measure the suspended particle size distribution in 32 logarithmically spaced size classes over the range 2.5 to 500 microns. Light is emitted by a laser diode with a wavelength of 670 nm and passes through a collimating lens, then through the 5 cm length sampling volume (Figure 7). After passing through a collimating lens, the scattered light is collected by a set of concentric ring detectors. Particles in the sampling volume refract the beam, forming a diffraction pattern on the ring. For simple geometries (spheres), the diffraction pattern can be predicted theoretically [Agrawal and Pottsmith]. The measured diffraction pattern, as sampled by the ring detectors, is then inverted to provide an estimate of the particle size distribution. The nature of forward scattering by spheres is such that the scattering angle is inversely proportional to particle diameter. Thus, the inner rings detect the largest particles, and the outer rings detect the smallest [Traykovski et al.]. Multiple diffractions can become a problem when total transmission is less than about 20-30% and results in a shift in the derived size distribution toward smaller size classes [Agrawal and Pottsmith]. The LISST instrument is commonly used by the oil industry in laboratory settings and was used heavily during our testing at Ohmsett [Belore et al.].

Figure 6. The precision acoustic instrument along with two acoustic transducers. The system is controlled via an Ethernet connection to the computer.

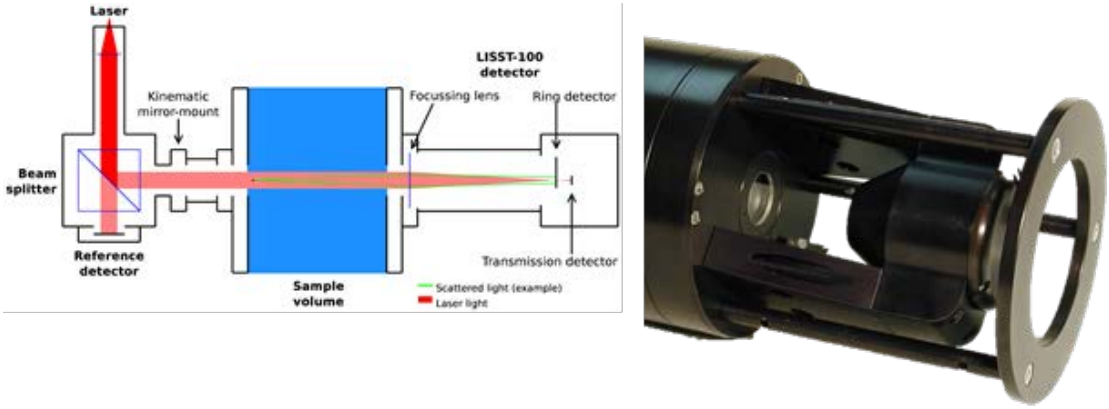

Figure 7. An optical schematic of the LISST is shown in the left panel. The right panel is a close up image of the sample volume.

We performed our lab measurements using two different experimental configurations. In the first configuration we simply mixed oil and dispersant in a plastic container filled with water using a paint mixer and a cordless drill. Photos of this setup are shown in Figure 8 for a small surface slick of 15 mL of Canadian Hebron oil before and after adding dispersant. For these measurements the LISST and the acoustic transducer were placed facing down in the small tank. Figure 9 shows the acoustic signals from the crude oil before and after adding Corexit 9500 at a dispersant-to-oil ratio (DOR) of 1:10. The LISST measurements were performed simultaneously with the acoustic measurements to benchmark the acoustics. During the initial experiments, our mixing was not optimum and the oil was allowed to age several hours prior to adding dispersant; thus, the oil droplet size remained above ~200 microns and did not disperse well. In addition, the paint mixer added many air bubbles into the mixture and distributed oil on the LISST windows and the sides of the container which further complicated our measurements.

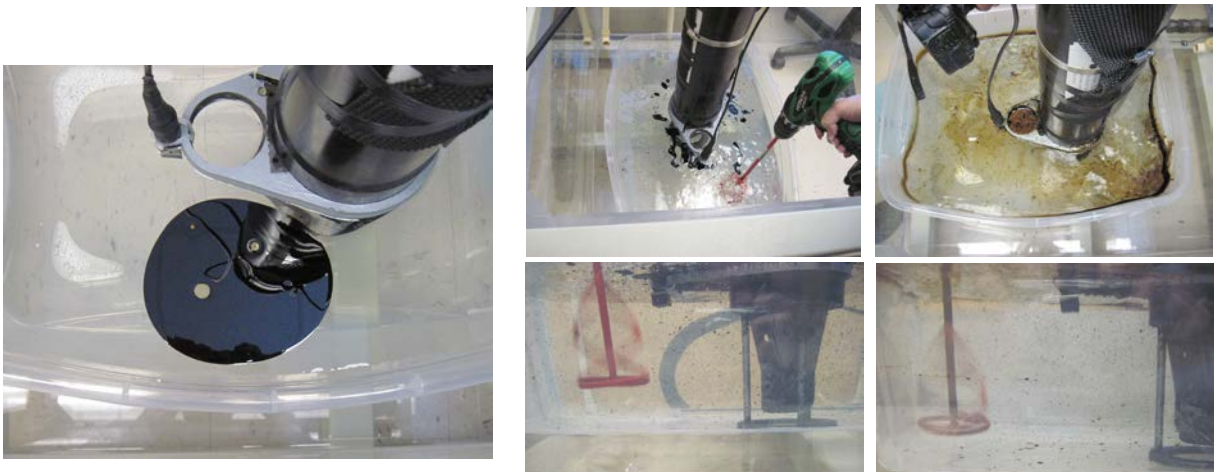

Figure 8. The left figure and two middle figures show 15 mL of Canadian Hebron oil in the test vessel prior to adding Corexit. The right two photos show the oil-water mixture after adding Corexit with a DOR of 1:2.5.

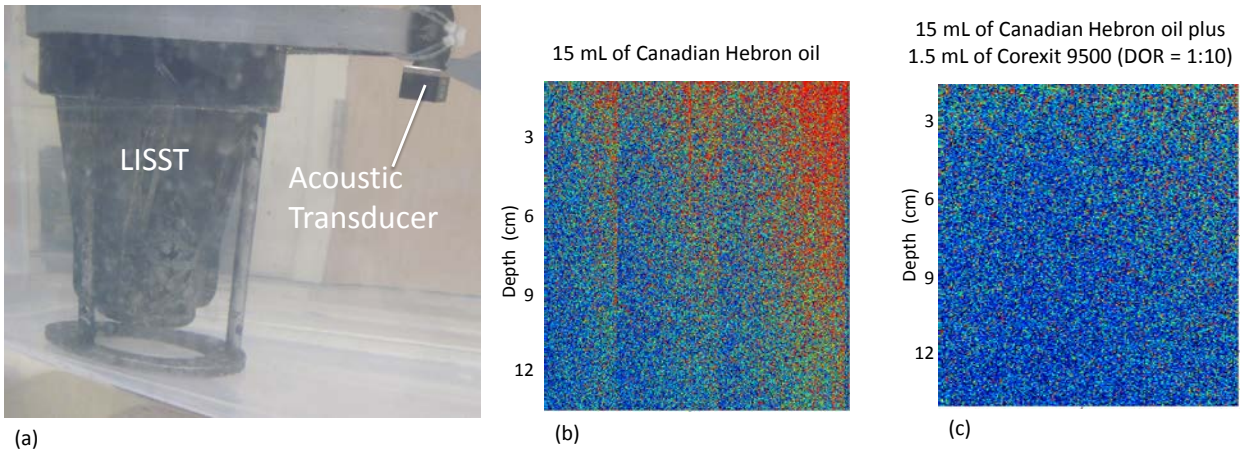

Figure 9. The left photo shows the LISST and acoustic transducer oriented down in the water tank. The acoustic backscattering signal are show in (b) for Hebron oil prior to adding dispersant, and in (c) after adding dispersant.

To overcome these issues, we moved to a more controlled setup, shown in Figure 10, where the oil and dispersant were mixed with a 60 mL syringe in a small measurement chamber which fit directly into the LISST measurement window. This setup enabled us to produce a well-mixed dispersion, control the introduction of air bubbles, and eliminate the contamination of the LISST optical windows with oil. We were also able to premix the oil and dispersant prior to adding them to the water to ensure proper dispersion. We found that if the water and dispersant are mixed together prior to adding the oil, the dispersant formed micelles with their hydrophobic tails facing inwards and the hydrophilic heads facing towards the water and thus did not disperse the oil [Lewis and Aurand, Nedwed]. Interestingly, the acoustic wave scattered from these micelles while the LISST did not sense them.

We performed measurements on Canadian Hebron Oil with Corexit 9500 dispersant at various DORs ranging from 1:40 to 1:5. Acoustic images of scattering from the oil dispersions are shown in Figure 11 for oil only in the top panel and oil + Corexit 9500 at a DOR of 1:5 in the bottom panel. The corresponding droplet size distributions from the LISST are in the right hand panels. For the oil only, the droplet size ranged between 90 and 50 microns over the time period we measured with the smaller droplets staying in suspension longer. It was surprising that the droplet size was so small for an oil only mixture. We attribute this to the sample chamber being contaminated with dispersants and soap from earlier experiments and cleaning. Even though the droplet size was smaller than expected, the data were useful for our purpose of developing droplet sizing algorithms and measurement methods. Similarly for the dispersant and oil mixture, the droplet size decreased with time over the two minute test period (bottom right panel in Figure 11). The improved suspension of the oil with dispersant is clearly evident in the two acoustic data panels. The oil continued to stay dispersed for many 10s of minutes for the dispersant-oil mixture. While these images are useful, it is more important to determine the oil droplet size directly in field environments. To this end we developed analysis methods to determine the oil droplet size from these and other acoustic data in the lab and at Ohmsett.

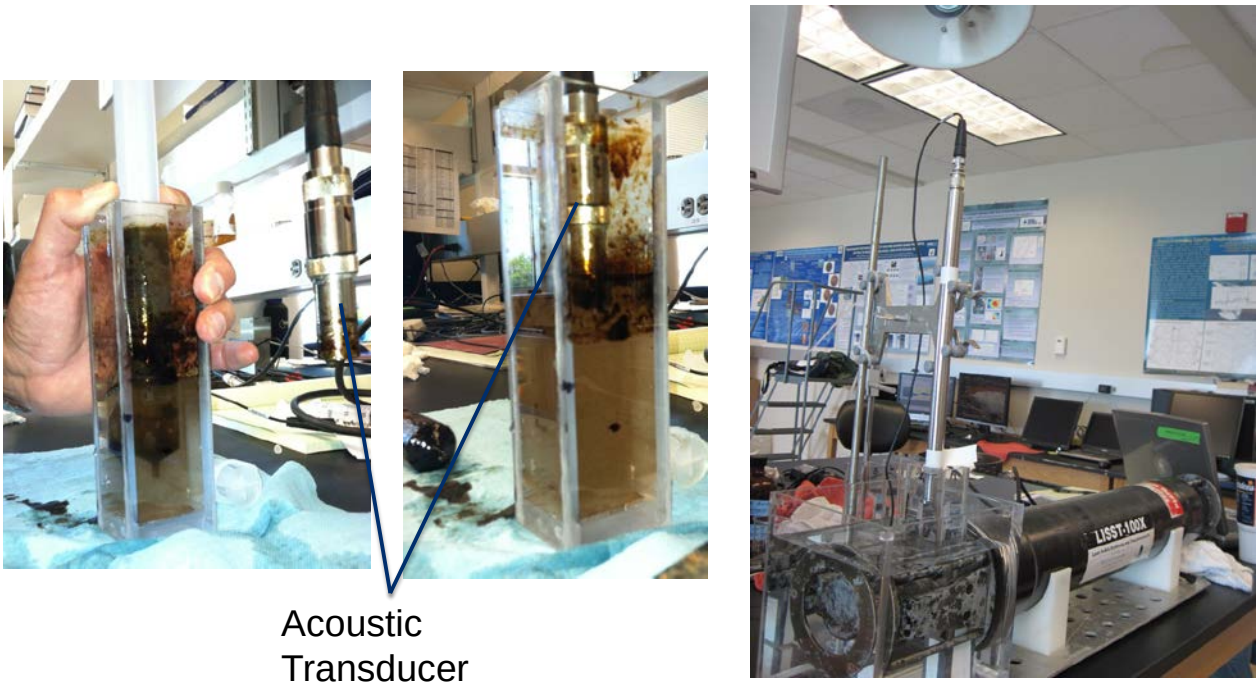

Figure 10. The acoustic test chamber for oil-dispersant mixtures. The syringe (left panel) was used to uniformly mix the suspensions. The acoustic transducer is shown pointing downward in the right panel.

Data were collected at 5 MHz in the lab and at Sintef, and at 1 MHz and 5 MHz at Ohmsett. As noted earlier, since 5 MHz was well above the resonant frequencies of these droplets, the relationship between the droplet size and acoustic attenuation was straightforward to interpret with the average droplet size proportional to the attenuation measured. At Ohmsett in August of 2012 it turned out that the runs were dominated by small droplets, with diameters less than 50 microns with a large number less than 10 microns. These small droplet sizes were not typical of any of our previous measurements. The large number of very small droplets created resonant scattering and absorption near 1 MHz, complicating the interpretation. This project was focused on the scattering effects only; thus, we developed our droplet sizing algorithms using the 5 MHz data. Interpreting the resonant effects and exploiting the resonant characteristics of oil and gas bubbles is the focus of the next phase of this project. In that work we plan to span frequencies that overlap directly with the resonant frequencies of oil droplets and gas bubbles.

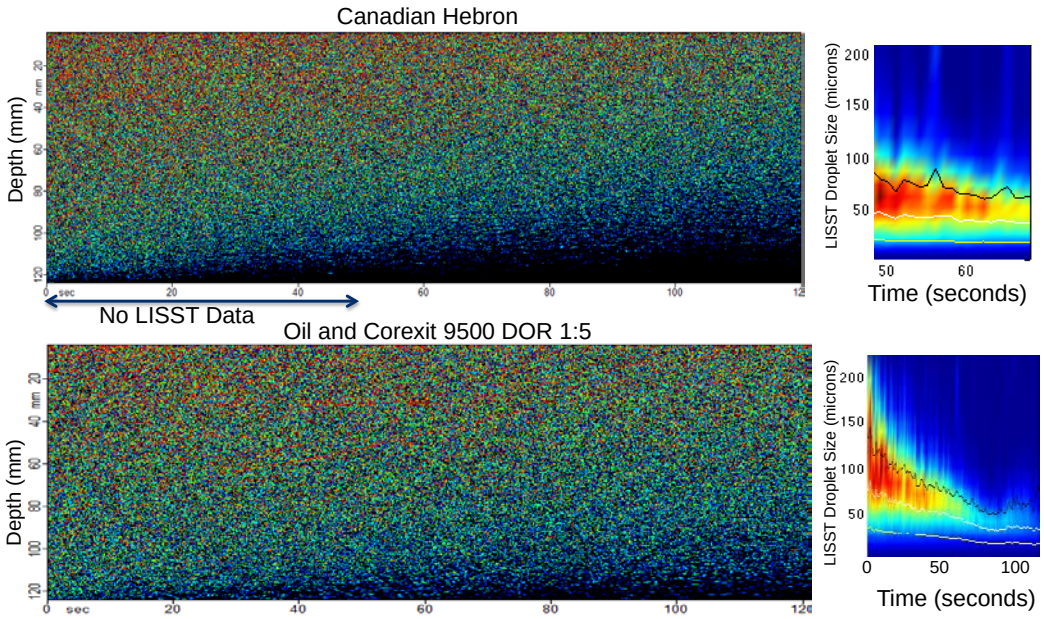

Figure 11 Acoustic backscattering for oil and oil-dispersant mixtures along with the associated droplet size distribution determined from LISST measurements vs., time. In each case red indicates a relatively stronger acoustic or LISST response.

3.3 TESTING AT OHMSETT

We accompanied ExxonMobil personnel during their dispersant testing at Ohmsett on two occasions during December 2011 and August 2012 for a total of 6 days of measurements. Figure 12 is an aerial photograph of the Ohmsett test facility. The goal of the tests in December 2011 on Canadian Hebron oil was to determine the best operating frequencies and how to configure the transducer with the LISST. In August 2012 we returned to Ohmsett for more in-depth testing including emulsified oils and two different dispersants, Corexit 9500 and ExxonMobil's gel dispersant. A description of data collected during each visit is provided in subsequent subsections.

3.3.1 December 2011 Ohmsett Testing

For our tests in December, we attached a 5 MHz ultrasonic sensor directly to Ohmsett's LISST. The sensors were inserted approximately 1 meter below the surface of the water from the Tow Bridge. Figure 13 shows these configurations. Once in the water, the acoustic transducer pointed upward, toward the surface of the water. With this configuration, we were able to observe scattered signals from approximately 1 meter deep (the sensor surface) to approximately 0.5 meters deep. Figure 14a shows the waves moving across the test tank prior to spilling the oil. Figure 14b is a view of the slick that formed after approximately 20 gallons of Canadian Hebron crude oil were sprayed on the surface of the water. Figure 15a shows the slick breaking up from an initial spray of the dispersant, and Figure 15b shows the well mixed oil after many breaking waves formed.

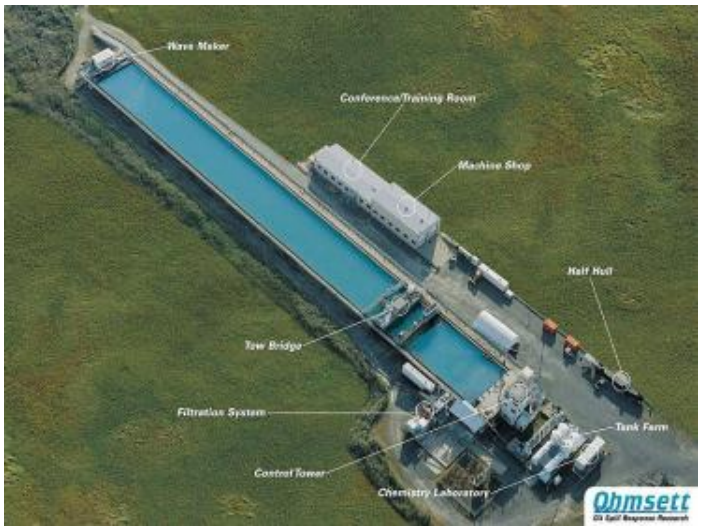

Figure 12. Aerial view of the Ohmsett facility. We set up on the tow bridge which moved along the tank during testing.

Figure 16a shows the background ultrasonic scattering prior to adding oil. For these measurements we collected 100 signals or "pings" over a 10 second period as the tow bridge was moved along the tank. The vertical axis is the distance from approximately 1 meter deep at the bottom of the figure to approximately 0.5 meters deep at the top. The horizontal axis is the time in seconds with each vertical trace being the returned signal from each ping. The color represents the amplitude of the returned signal with black being zero and red representing a high backscattered signal. Figure 17b shows the returned signal after adding Corexit 9500 with a DOR of 1:20 but with no breaking waves to mix up the oil and dispersant. There is essentially no difference because no turbulent mixing was occurring to mix up the oil and dispersant. Once the waves began breaking, the oil began to disperse below the surface. An acoustic "snapshot" of this dynamic process is shown in Figure 17a. Scattering from oil droplets can be seen as green to red pixels with the background being black to blue. There is variation in scattering signal in the image going from left to right and top to bottom, indicating the oil droplet concentrations and sizes were varying in the volume measured.

Figure 13. The ultrasonic transducer was zip tied to the LISST as shown in the left photograph and both sensors were submerged into the tank from the Tow Bridge as shown in the right hand photograph.

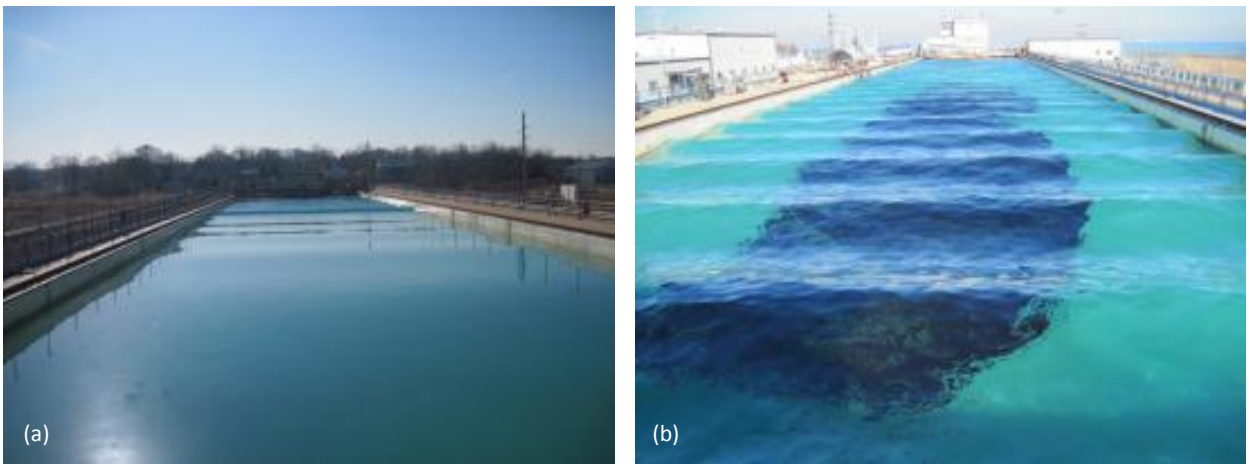

Figure 14. View from the Tow Bridge, (a) towards the wave maker and (b) the slick looking away from the wave maker.

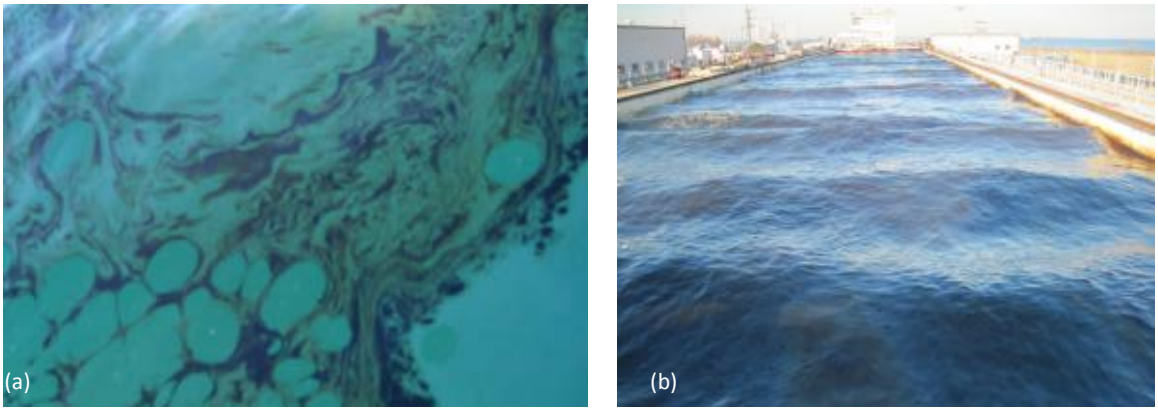

Figure 15. Images of the oil slick, (a) as dispersant is sprayed and (b) after many breaking waves mixed the oil and dispersant well.

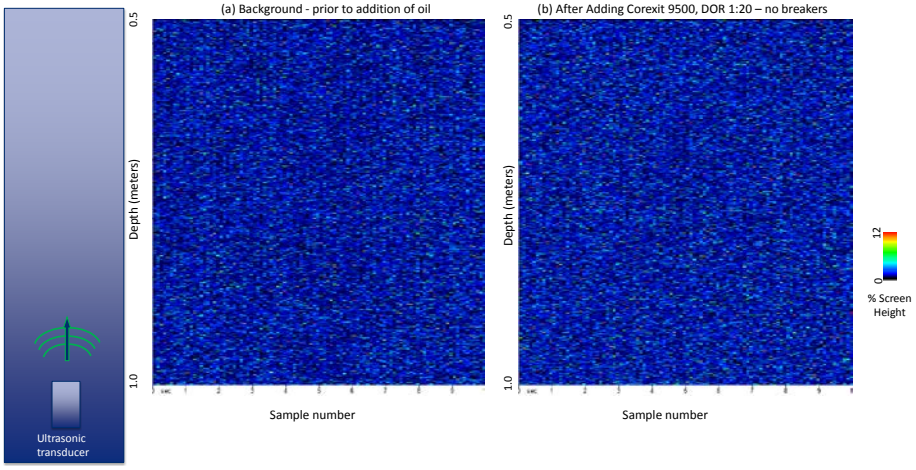

Figure 16. Acoustic images of the Ohmsett water column. (a) Background acoustic scattering in the water column prior to adding oil. (b) After Corexit is added but the oil is not dispersed. A schematic of the transducer is in the left hand panel shows the sound wave propagating up into the water column.

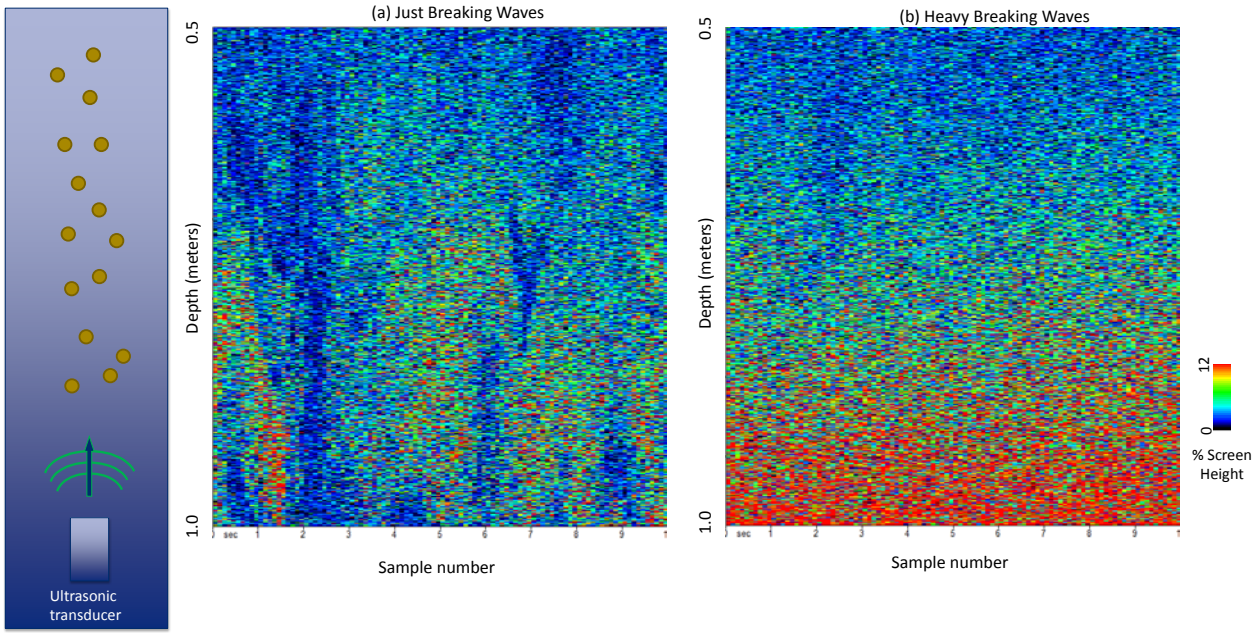

Figure 17. (a) Ultrasonic images of the Ohmsett water column as the waves begin to break and disperse the oil and (b) after many breaking waves dispersed the oil in the water column. The inhomogeneous mixing can be seen by the variability from left to right across the image in (a). The backscattering after strong mixing is high near the transducer as seen at the bottom of (b), then decreases with distance away from the transducer due to attenuation.

Once breaking waves formed, the mixing was improved as can be seen in Figure 17b where the backscattered amplitude profile with depth is uniform as a function of position, with the largest signals observed close to the ultrasonic sensor near 1 meter deep. The smaller signals approaching 0.5 meters deep do not necessarily indicate a lower oil concentration or smaller particle size near the surface, as might be expected. This change is due to the high attenuation at 5 MHz. Scattering and absorption processes attenuated the signal as the wave traveled away from the transducer (up the page) and then returned to the same transducer (down the page) after scattering from the droplets. As discussed in the previous section of this report, the measurements in December 2011 were very successful in helping to determine the frequency range where useful data can be obtained. Based on these data, we determined that 5 MHz is good for both visualizing dispersed oil for surface applications and determining the droplet size. The decrease in signal at 5 MHz was desirable since it allowed us to measure the attenuation and stay well above the resonant frequencies of the droplets which can complicate the interpretation of the scattering results.

3.3.2 August 2012 Ohmsett Testing

We returned to Ohmsett in August 2012 for testing on a variety of oils with two dispersants - Corexit 9500 and ExxonMobil's gel dispersant. The experimental runs are summarized in Table 2. We collected acoustic data on all runs except Run 11. For these tests we brought several acoustic transducers including 500 kHz, 1 MHz, 2.25 MHz, 5 MHz and 10 MHz transducers. In addition, we brought the VIMS LISST, a commercial sonar system from Imagenex that operates at frequencies from 350 kHz to 1 MHz, and a commercial Sontek Acoustic Doppler Velocimeter (ADV) operating at 5 MHz. Photographs of the LISST with the sonar and acoustic transducers attached are shown in Figure 18. For simplicity, we zip tied and taped the sonar and acoustic transducers onto the LISST. With this configuration we only needed to lower one instrument cluster into the water and could be confident that the LISST, sonar and acoustic transducers were sampling similar regions in the plume.

The Sonar and ADV (Figure 19) were only used intermittently throughout the week because their acoustic pulses interfered with our acoustic reception. The assessment of these two instruments will be discussed in subsequent sections. Figure 20 shows the suite of instruments during deployment from the bridge and the final position in the tank. The low signal-to-noise ratio for the 500 kHz measurements and the 10 MHz transducers caused the data to not be usable, and the 2.25 MHz transducer had a frequency bandwidth that overlapped with the 1 MHz and 5 MHz transducers. Thus, we focused our measurements and analysis on the 1 MHz and 5 MHz acoustic transducers.

Table 2 Description of oil and dispersants used during the testing at Ohmsett in August 2012.

Run #	Day	Date	Location	Mixing	Oil	Dispersant	DOR	Acoustics	Sonar	ADV
Run 1	Monday	August 13, 2012	Ohmsett	Waves	Endicott - Fresh	None		✓		
Run 2	Monday	August 13, 2012	Ohmsett	Waves	Endicott - Fresh	Corexit 9500	1:20 (10 gallons oil, 1/2 gallon Corexit)	✓	✓	
Run 3	Tuesday	August 14, 2012	Ohmsett	Waves	Venoco E19 Emulsion	Corexit 9500	1:10	✓		
Run 4	Tuesday	August 14, 2012	Ohmsett	Waves	Venoco E19 Emulsion	Corexit 9500	1:40	✓		
Run 5	Wednesday	August 15, 2012	Ohmsett	Waves	Venoco E19 Emulsion	ExxonMobil Gel	1:40 (2 gallons Gel)	✓	✓	✓
Run 6	Wednesday	August 15, 2012	Ohmsett	Waves	Venoco E19 Emulsion	ExxonMobil Gel	1:10 (2 gallons Gel)	✓	✓	✓
Run 7	Wednesday	August 15, 2012	Ohmsett	Waves	Venoco E19 Emulsion	Corexit 9500	1:10	✓	✓	✓
Run 8	Thursday	August 16, 2012	Ohmsett	Waves	Sockeye Emulsion	Corexit 9500	1:20 (16.6 gallons oil, 0.759 gallons Corexit	✓	✓	✓
Run 9	Thursday	August 16, 2012	Ohmsett	Waves	Sockeye Emulsion	ExxonMobil Gel	1:20 (15.9 gallons oil, 0.75 gallons Gel)	✓	✓	✓
Run 10	Thursday	August 16, 2012	Ohmsett	Waves	Endicott Emulsion	ExxonMobil Gel	1:14 (21 gallons oil, 1.5 gallons Gel - 0.5 second application)	✓	✓	✓
Run 11	Friday	August 17, 2012	Ohmsett	Waves	Endicott Emulsion	Corexit 9500	1:20			
Run 12	Friday	August 17, 2012	Ohmsett	Waves	Endicott Emulsion	ExxonMobil Gel	1:20 (22 gallons oil, 1 gallon Gel)	✓	✓	✓

Figure 18 The configuration of the LISST, Sonar and acoustic transducers prior to deployment.

During the first day we were able to collect data on fresh Endicott oil both with and without dispersants. Figure 21 shows the oil in the tank before and after dispersant application. During the week we made measurements on several emulsified oils as indicated in Table 2. A representative photograph of one of the emulsified oils is shown in Figure 22 before and after the application of dispersant. These oils and treatments were chosen by ExxonMobil to test the efficacy of their new gel dispersant relative to the industry standard Corexit 9500.

Figure 19. ADV used at Ohmsett. The transducers have yellow faces. The center transducer emits the sound and the outer three transducers receive the sound waves scattered from particulates in the water column.

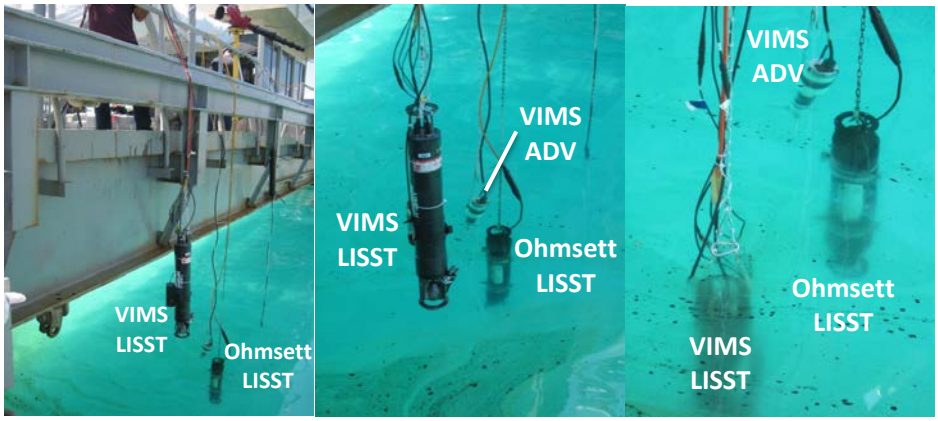

Figure 20 These photographs show the VIMS LISST as it is being deployed over the railing of the bridge along with the Ohmsett LISST. The center and right photographs show the two LISSTs along with the VIMS ADV.

For these tests, we moved the transducers closer to the surface relative to the December 2011 tests, so we could image the water column all the way to the surface of the water. One example of the background without oil showing the waves on the surface of the water over a 30 second time period is presented in Figure 23. A schematic of the transducers is on the left pointing up toward the surface of the water. Here black is low amplitude and red is high amplitude. This is the same type of image produced by commercial sonar; however, we have access to the full acoustic waveform which we used to determine the droplet size. The wave surface is clearly visible as the sensor moves through the water from left to right. Our sensors measured the wave height from crest to trough to range from 20 to 35 cm. This height agreed with visual determinations made during testing as well as the target wave height set by the Ohmsett staff. Once oil and dispersants were added and waves began to break, the scattering from oil in the water column was significant as shown in the bottom image of Figure 23. This image shows the acoustic backscattering from the upward looking transducer over a 2 minute period with each ping occurring every 0.1 seconds. The waves are visible and ranged from 15 cm to over 50 cm. The bright red regions near 60 seconds, 85 seconds, and from 95 to 110 seconds indicate a high density of oil dispersed deep into the water column. Breaking waves are visible as bluish-red above 800 mm from the surface of the transducer. When these waves break, oil and air get

Figure 21 Photographs of Run 1 using fresh Endicott crude oil before (left) and after (right) addition of dispersant. The right photograph shows our instruments directly in the plume.

Figure 22. Photographs of one of the emulsified oils in the Ohmsett tank (top left), personnel from S.L. Ross applying dispersant using a pump sprayer (top right) and the emulsified oil after the dispersant was applied (bottom).

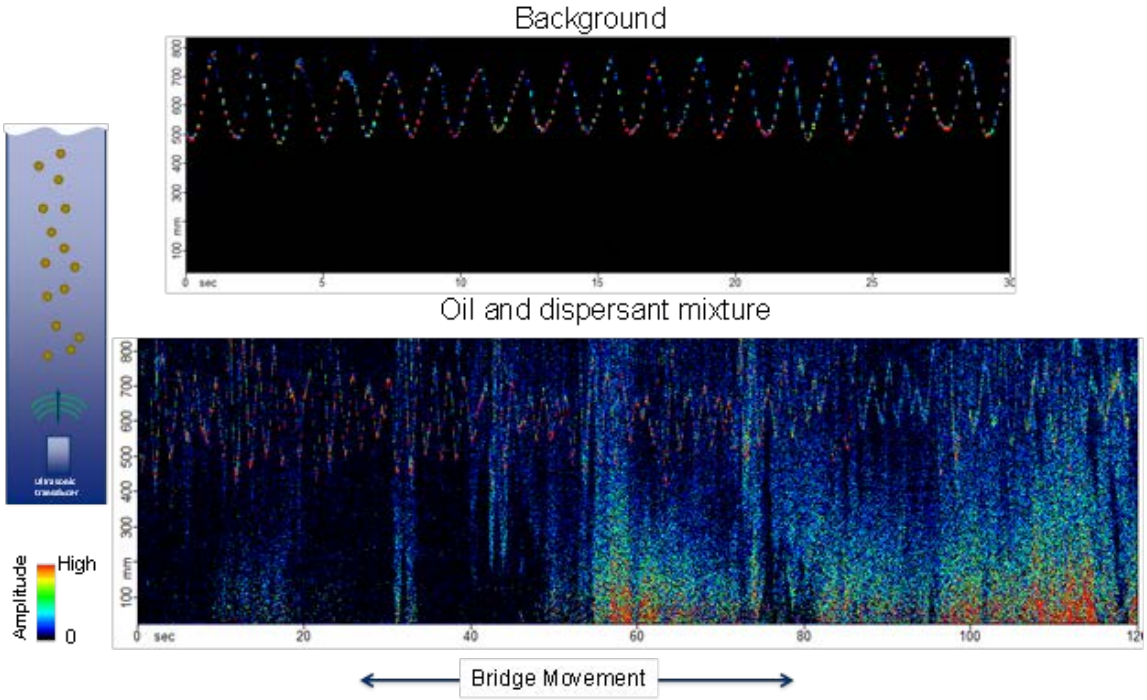

Figure 23 Typical acoustic scattering results from August 2012 testing at Ohmsett. The top figure is the background prior to oil addition. The bottom figure is after oil and dispersants were added.

dispersed into the water column. Visualizations of this are seen in the acoustic backscattered signal near 35 seconds, 40 seconds, 60 seconds, 75 seconds, and above 90 seconds. Our acoustic measurements are very good at visualizing the oil and air in the water column with a higher resolution than commercial sonar. Where we differ even more markedly is in our ability to analyze the raw acoustic signal in the frequency domain to determine the oil droplet size, as described in the next section of this report.

3.4 Acoustic Determination of Oil Droplet Size

While sonar instruments are very good at visualizing oil in a water column, we have gone beyond imaging and developed methods to directly measure the oil droplet size in-situ. This section describes the method used to determine the droplet size from acoustic data. There are several steps in the process to ensure good benchmark data and registration between the LISST measurements of the droplet size distribution and our acoustic data. First, the oil concentration needed be above ~ 20 ppm for accurate droplet size distribution calculations. Figure 24 shows the results from the LISST

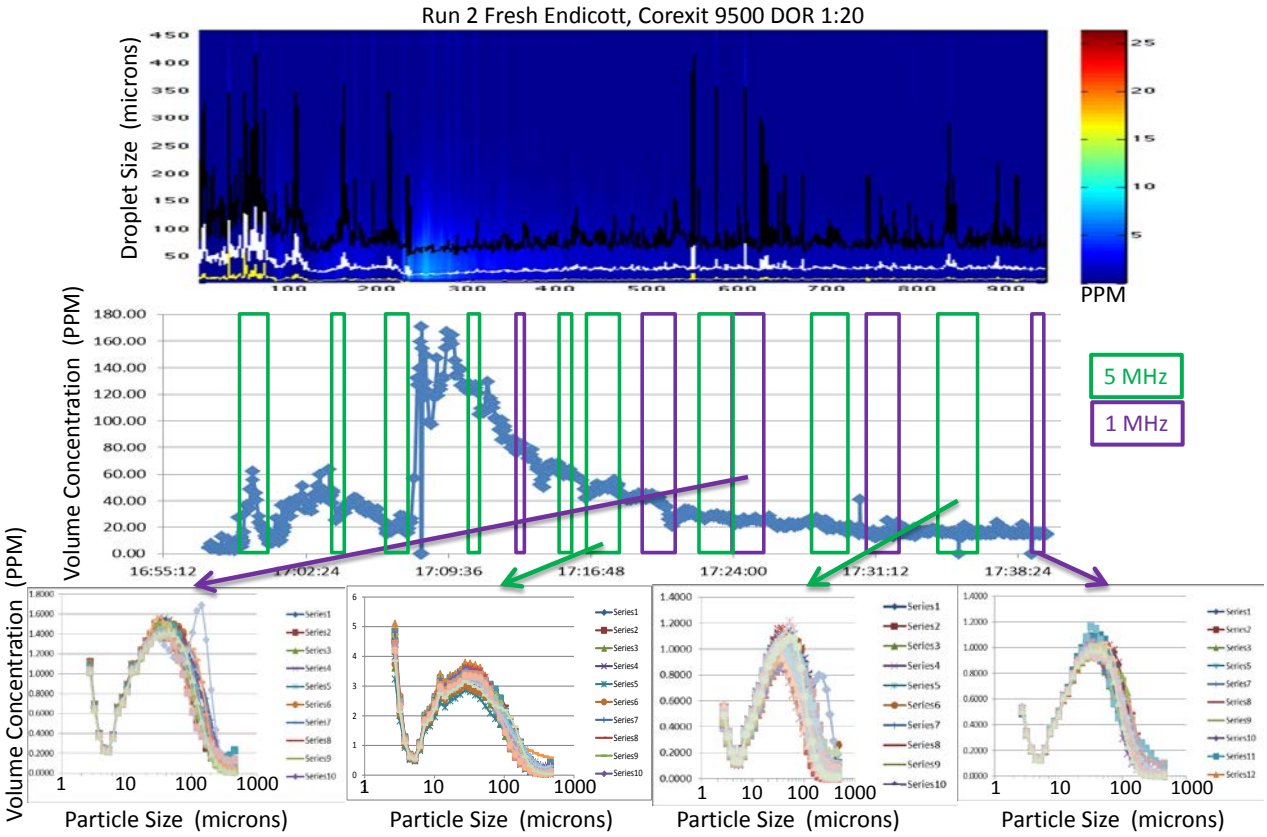

Figure 24 LISST data showing the droplet size in the top panel, the concentration in the middle panel, and the droplet size distributions in the lower panels. The lines on the top figure show the D84 in black, D50 in white, and the D16 in yellow, where the number indicates the % of droplets below the number.

measurements for Run 2 using fresh Endicott and Corexit 9500 at a DOR of 1:20. The top figure shows the droplet size as a function of sample number, or time, with red being a high concentration and black being low concentration for that particular record. The middle figure shows the volume concentration for all droplet sizes in each record as a function of time. We have found the LISST was unreliable when the concentration was below about 20 ppm or above about 500 ppm.

The green and purple boxes in the middle panel show the regions where acoustic data were collected. Acoustic data were collected at 1 MHz in the green boxed regions and at 5 MHz in the purple boxed regions. The corresponding acoustic scattering is shown in Figure 25 for 1 MHz and Figure 26 for 5 MHz in the time windows indicated in the figures. Data were collected every 0.1 seconds as the bridge was moved up and down the Ohmsett wave tank. We calculated the acoustic attenuation from the measured backscattering signals and compared the attenuation with average droplet size in those particular time regions. By correlating all of the LISST data with the acoustic data as just described we were able to select specific runs for comparison with the LISST droplet size. The green highlighted rows in Table 3 are the runs where we both collected data at 5 MHz and have usable LISST droplet size distributions.

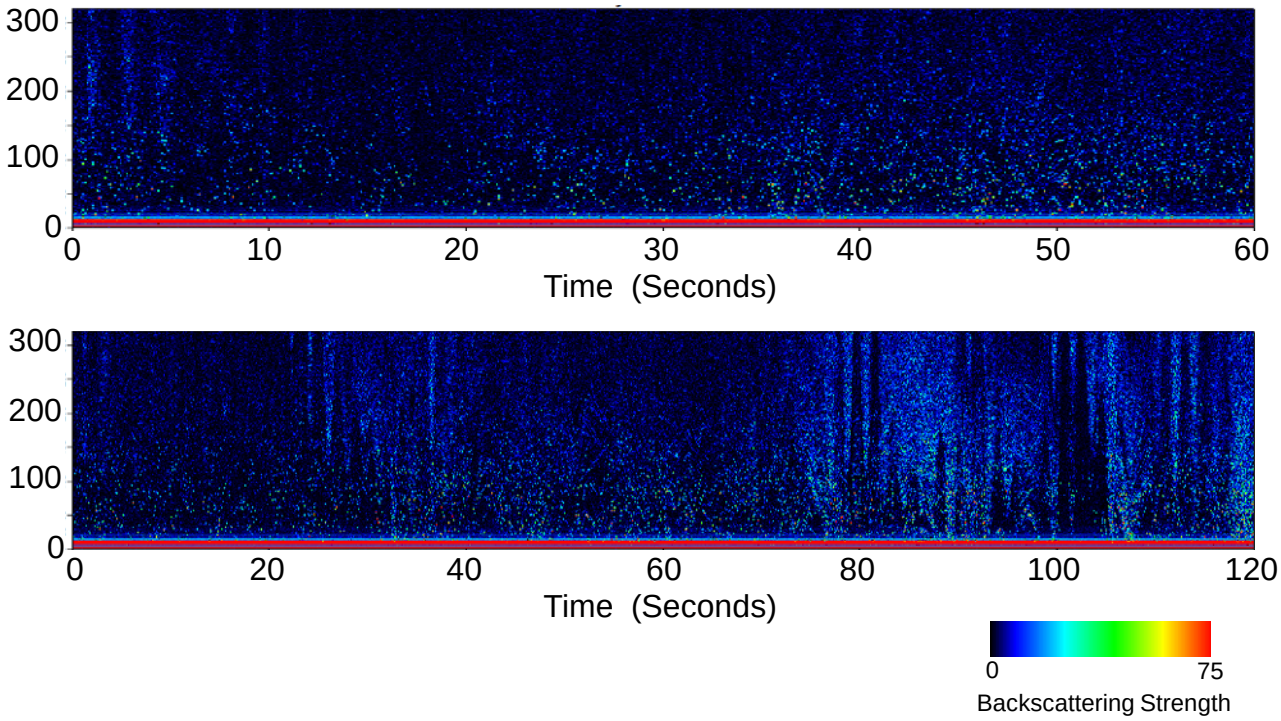

Figure 25. Acoustic scattering at 1 MHz in two regions during Run 2. Data were collected every 0.1 seconds for 60 seconds in the top image and 120 seconds in the bottom image.

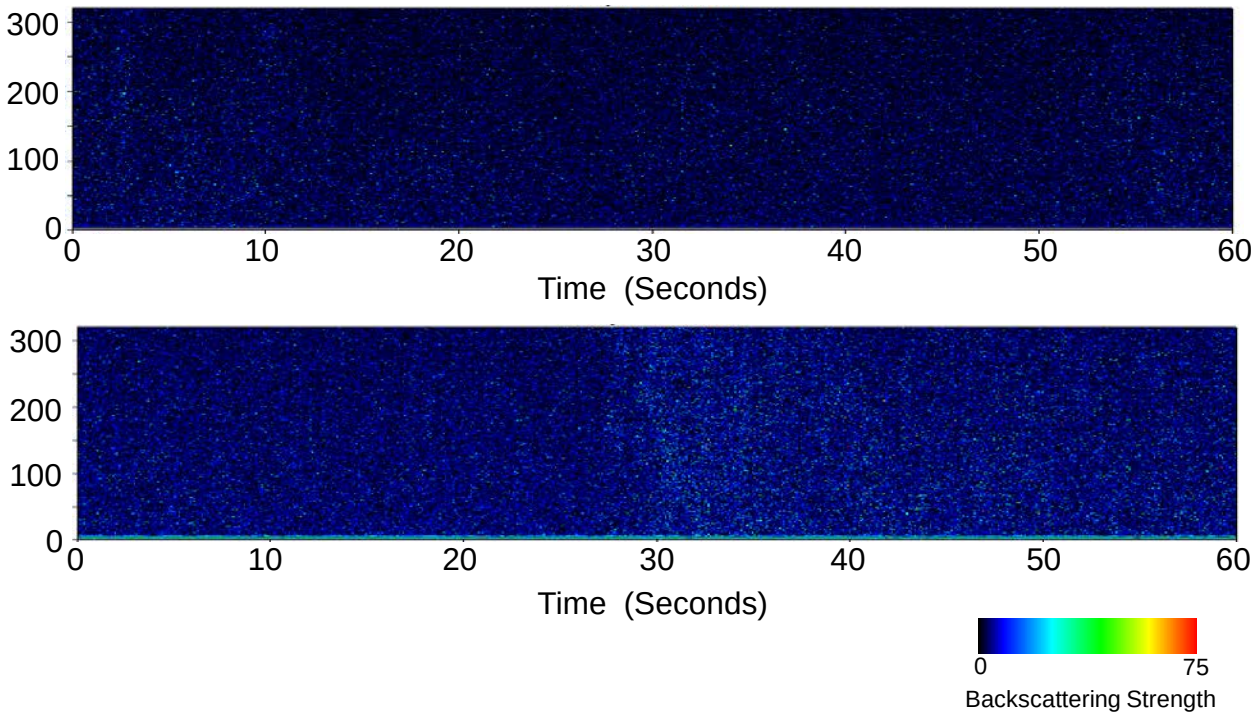

Figure 26. Acoustic scattering at 5 MHz in two regions starting at 17:11 and 17:14 in Run 2. Data were collected every 0.1 seconds for 60 seconds.

Table 3. Identification of data used from August 2012 Ohmsett runs for calibration. All data have been analyzed. The data from the green highlighted regions is presented in the body of the report.

Run #	Day	Date	Location	Mixing	Oil	Dispersant	DOR	Acoustics	Sonar	ADV
Run 1	Monday	August 13, 2012	Ohmsett	Waves	Endicott - Fresh	None		✓		
Run 2	Monday	August 13, 2012	Ohmsett	Waves	Endicott - Fresh	Corexit 9500	1:20 (10 gallons oil, 1/2 gallon Corexit)	✓	✓	
Run 3	Tuesday	August 14, 2012	Ohmsett	Waves	Venoco E19 Emulsion	Corexit 9500	1:10	✓		
Run 4	Tuesday	August 14, 2012	Ohmsett	Waves	Venoco E19 Emulsion	Corexit 9500	1:40	✓		
Run 5	Wednesday	August 15, 2012	Ohmsett	Waves	Venoco E19 Emulsion	ExxonMobil Gel	1:40 (2 gallons Gel)	✓	✓	✓
Run 6	Wednesday	August 15, 2012	Ohmsett	Waves	Venoco E19 Emulsion	ExxonMobil Gel	1:10 (2 gallons Gel)	✓	✓	✓
Run 7	Wednesday	August 15, 2012	Ohmsett	Waves	Venoco E19 Emulsion	Corexit 9500	1:10	✓	✓	✓
Run 8	Thursday	August 16, 2012	Ohmsett	Waves	Sockeye Emulsion	Corexit 9500	1:20 (16.6 gallons oil, 0.759 gallons Corexit	✓	✓	✓
Run 9	Thursday	August 16, 2012	Ohmsett	Waves	Sockeye Emulsion	ExxonMobil Gel	1:20 (15.9 gallons oil, 0.75 gallons Gel)	✓	✓	✓
Run 10	Thursday	August 16, 2012	Ohmsett	Waves	Endicott Emulsion	ExxonMobil Gel	1:14 (21 gallons oil, 1.5 gallons Gel - 0.5 second application)	✓	✓	✓
Run 11	Friday	August 17, 2012	Ohmsett	Waves	Endicott Emulsion	Corexit 9500	1:20			
Run 12	Friday	August 17, 2012	Ohmsett	Waves	Endicott Emulsion	ExxonMobil Gel	1:20 (22 gallons oil, 1 gallon Gel)	✓	✓	✓

Figure 27 shows the average droplet size from the LISST vs. the acoustic attenuation for data collected at Ohmsett in 2011, in the lab, and at Ohmsett in 2012. The blue circles are the data used for the calibration curve. The purple squares are the attenuation for Dorado oil collected in our lab in December 2012. The physics governing this attenuation as a function of scatterer size is detailed in many publications [Urick, Medwin] and the work by our members of our project team [Panetta et al. 2002, Panetta et al. 2003, Panetta 2010, Panetta et al. 2012]. At 5 MHz, the acoustic attenuation can be directly related to the average droplet size through the relationship shown in Figure 27, where the average droplet size determined from the LISST is plotted vs. the acoustic attenuation for the laboratory and both trips to Ohmsett. In general the data fit well except for the Dorado oil measured in the lab. The low viscosity of the Dorado oil may be contributing the poor fit. Since all of our measurements were on higher viscosity oils or emulsified oil, we may need to expand our database and theoretical knowledge to incorporate a wider range of viscosities.

Using the linear relationship in Figure 29 (excluding the Dorado oil), we calculated the expected droplet size based on our acoustic measurements of attenuation at 5 MHz. The acoustically determined droplet size vs. the LISST measurement of the droplet size is plotted in Figure 28. The black line shows the perfect 1:1 correspondence between the measurements. Even with the scatter around the ideal fit the trend is clear. Additional measurements with a wider range of oils are needed to statistically validate the relationship. However, these results are very encouraging and are a significant step toward developing the field measurements of oil droplet size using acoustic scattering

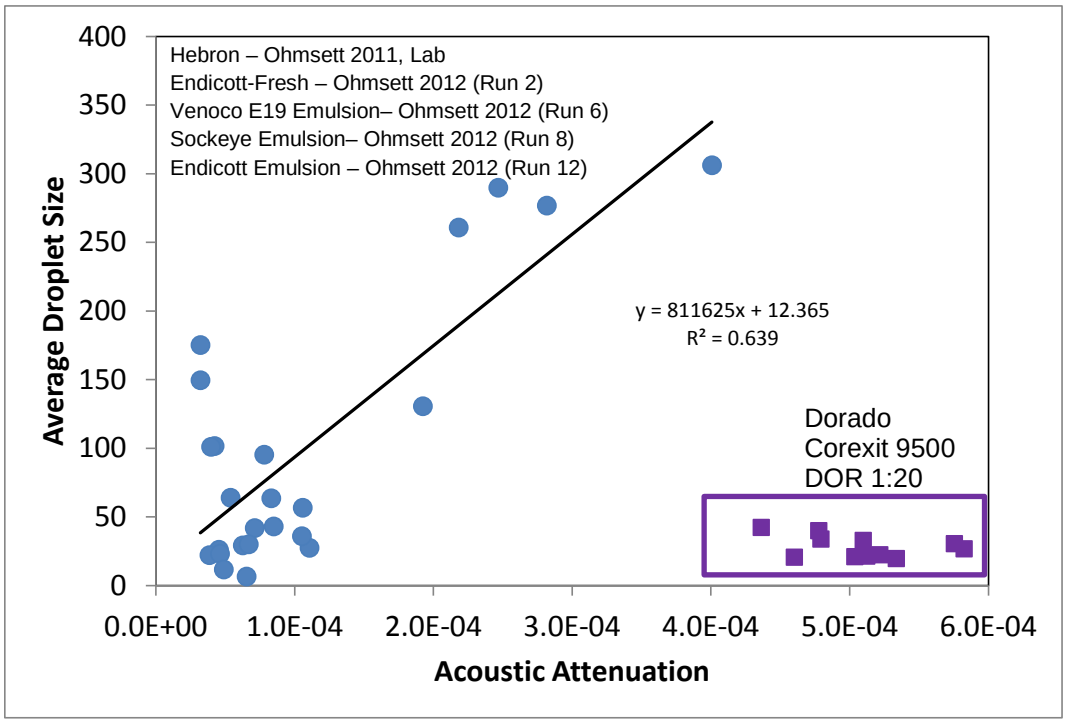

Figure 27. The mean droplet size measured by the LISST vs. the acoustic attenuation for the Ohmsett 2011, laboratory measurements, and Ohmsett 2012 data.

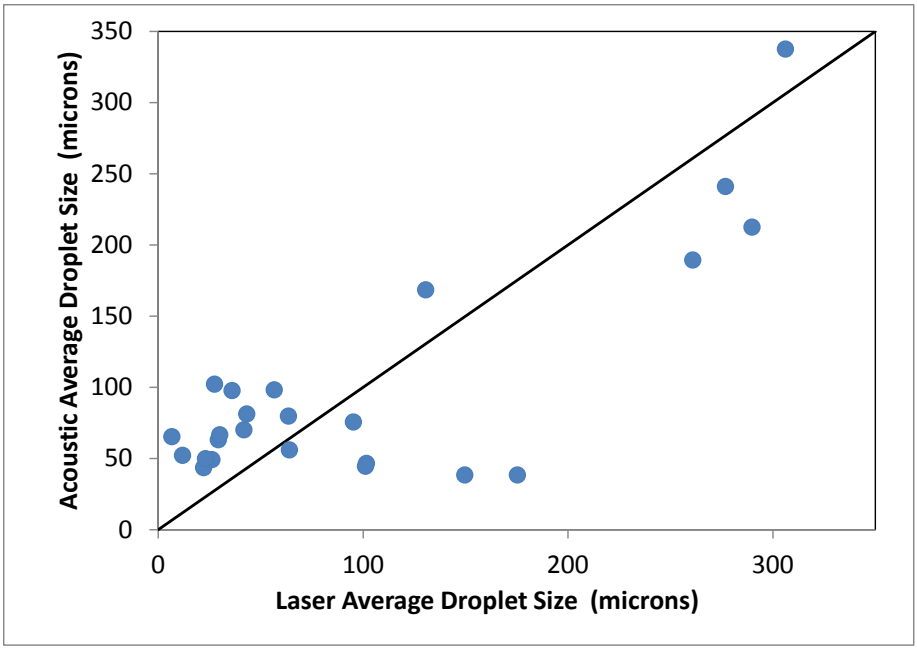

Figure 28. Acoustically determined droplet size vs. the average droplet size determined by the LISST.

3.5 Assessment of Commercial Sonar and ADV Instruments

As part of this work we assessed the potential for commercial sonar and marine acoustic instruments to measure oil droplets in water. The goal of this task was simply to determine if they could be used without modification to measure oil droplet size or accelerate the transfer of the technologies we are developing into commercial instrumentation for oil spill response. We chose to evaluate the aforementioned Sontek ADV, which operates at 5 MHz, and the Imagenex imaging sonar system that operates between 350 kHz and 1 MHz.

3.5.1 ADV Assessment

The Sontek ADVOcean operates at 5 MHz in a bistatic configuration, i.e., separate acoustic transducers are used to transmit and receive sound waves. The geometry of the three receivers in relation to the transmitter creates a fixed remote sample volume (Figure 29), which ensonifies a single point located 18 cm from the transmitting transducer. The ADV is predominantly used to measure currents using the Doppler shift of the acoustic waves scattered from suspended particulates. If the particulates are moving toward the transducers, the acoustic frequency of the scattered wave gets shifted higher than the transmitted signal. In contrast, if the particulates are moving away from the transducers, the frequency of the scattered wave is lower than the transmitted signal. By monitoring the difference of the frequencies between the transmitted and received signals, the instrument can determine the speed and direction of the particulates and thus the current velocity [Sontek].

Figure 29. Images of the Sontek ADV are shown with propagation of the sound waves shown at left and a photograph of the entire instrument shown at right.

The ADV has long been used to measure current velocity in marine environments. Because the ADV signal is generated by scattering from suspended particulates, it has also been used to measure the concentration of suspended particulate matter [Lohrmann] and by our team [Cartwright et al.] based on the strength of the scattered signal. Because the ADV measures the backscattering at the same frequency we have been using, it was a natural choice for evaluation during the Ohmsett testing in August 2012. We measured the strength of the backscattered signal on seven runs. Data collected for Runs 5 and 6 are shown in Figure 30 and Figure 31, respectively. During Run 5 data were collected for a little less than 1 minute while during Run 6 data were collected for approximately 21 minutes. The figures show the average number of backscattering counts received at the three sensors over time as the bridge moved back and forth along the tank. During Run 5 the backscattering was at the background level of ~ 37 for the first 20 seconds then increased to approximately 45 counts for the last 20 seconds of the measurement time, indicating that oil droplets in the water scattered sound back to the transducers. During Run 6, the ADV showed many excursions above the background noise level, reaching backscattering counts well above 70 about 12 minutes into the run and above 80 counts during the last 5 minutes of the run. The intermittent high backscattering occurred when the instrument moved into the oil.

The ADV can certainly detect particulates in the water column. But the instrument only provides the backscattered amplitude which is affected by both the number of droplets and the droplet size. Without the full acoustic waveform, it would be difficult to use the instrument for measuring droplet size. However, there are additional modes of operation and other instruments from Sontek that can be explored. Furthermore, with modifications, it has the potential to be a useful instrument if full waveform can be provided for analysis. These alterations would require significant changes to the instrument. During discussions with Sontek representatives, they have expressed an interest in exploring these modifications if there is interest from the oil spill response community in the completed instrument. We recommend continuing to assess Sontek instruments and discussing options with Sontek for future technology transfer.

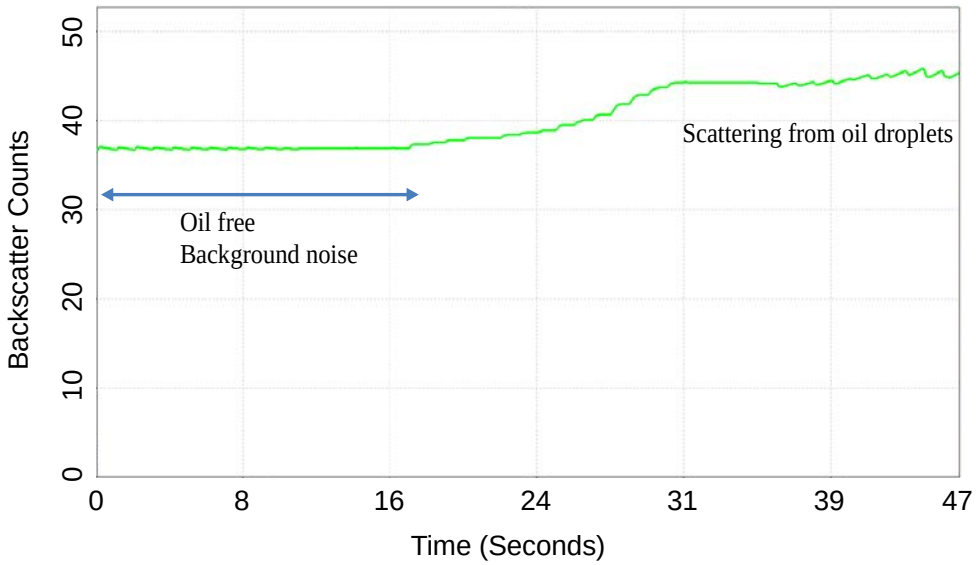

Figure 30 Backscattering measured by the Sontek ADV over a 47 second period showing a transition from an oil free region to a region with scattering from suspended oil.

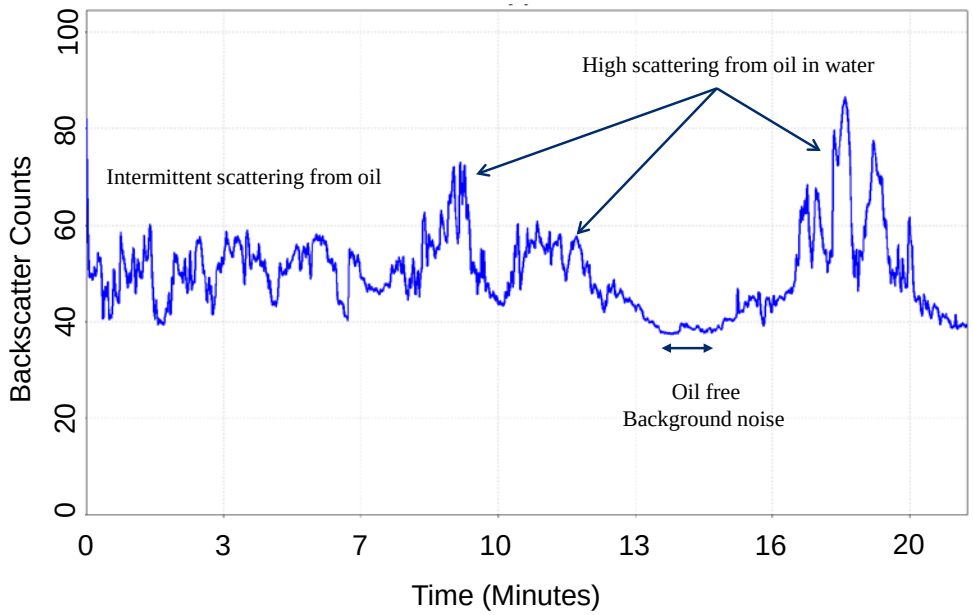

Figure 31. Backscattering amplitude from the Sontek ADV over a 21 minute time period for Run 6 at Ohmsett in August 2012. The background is at approximately 37 counts.

3.5.2 Imagenex Rotory Sonar Assessment

The Imagenex 881a is a multi-frequency rotary digital imaging sonar. The default frequency settings are 310 kHz, 675 kHz, or 1 MHz. However, it is tunable from 280 kHz to 1.1 MHz in 5 kHz steps using programmable software configurations. This sonar measures the distance between a source and a reflector (or scatterer such as an oil droplet) based on the echo return time. The 881a scans an area by rotating a

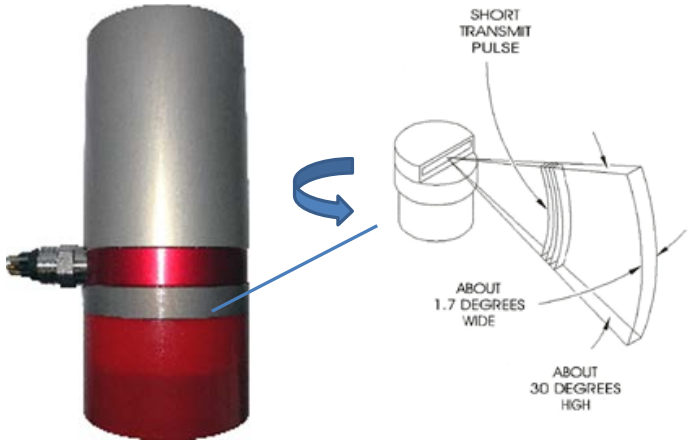

Figure 32. The Imagenex 881a sonar. The transducer is inside the red housing and rotates around the long axis of the sensor, emitting a fan shaped beam.

transducer which produces a fan-shaped sonar beam through a series of small steps, as shown in Figure 22 The transducer is housed in the red region of the sensor and rotates around the vertical axis. It was designed to scan at shallow angles, usually through a horizontal angle. It displays circular color images, or pie shaped portions, made up of a series of different colored points along a series of lines. The colors along these lines depict the return strengths of echoes from sonar beams as the acoustic transducer rotates. The distance from the center of the image represents the time for each echo to return, and the angle around the circle represents the directional orientation of the sonar beam. With the proper visual images, the operator can recognize sizes, shapes and surface reflecting characteristics of a chosen target. The primary purpose of the imaging sonar is as a viewing tool [Imagenex, 2004]. We tested this sonar system because the frequency range spans a wide range and enters into the range that we are currently using. In addition, its frequency range is near the resonant frequency of some of the smaller droplets we expect to see.

We tested the rotary sonar on Ohmsett Runs 5 through 12, excluding Run 11. Two representative examples are shown in Figure 33 and Figure 34 at 1 MHz and 350 kHz respectively. The sonar image is shown in the left panel and the acoustic scan at 1 MHz is shown in the top right panel with the corresponding droplet size from the LISST below it. The time displayed in the sonar image corresponds to one ping within the yellow box in the acoustic image on the top right. Each red ring is 0.2 meters from the sonar face. Figure 33, at 1 MHz, shows moderate scattering in the sonar image and our acoustic image. In both images red is high scattering and black is low scattering. In this particular scan we rotated the transducer halfway around to avoid interference with the LISST. In Figure 34, at 350 kHz, the scattering was significantly higher in both the sonar image and our acoustic image indicating there was a significant amount of oil dispersed in the water column. The droplet size determined by the LISST distribution is inconclusive and is very broad in this region.

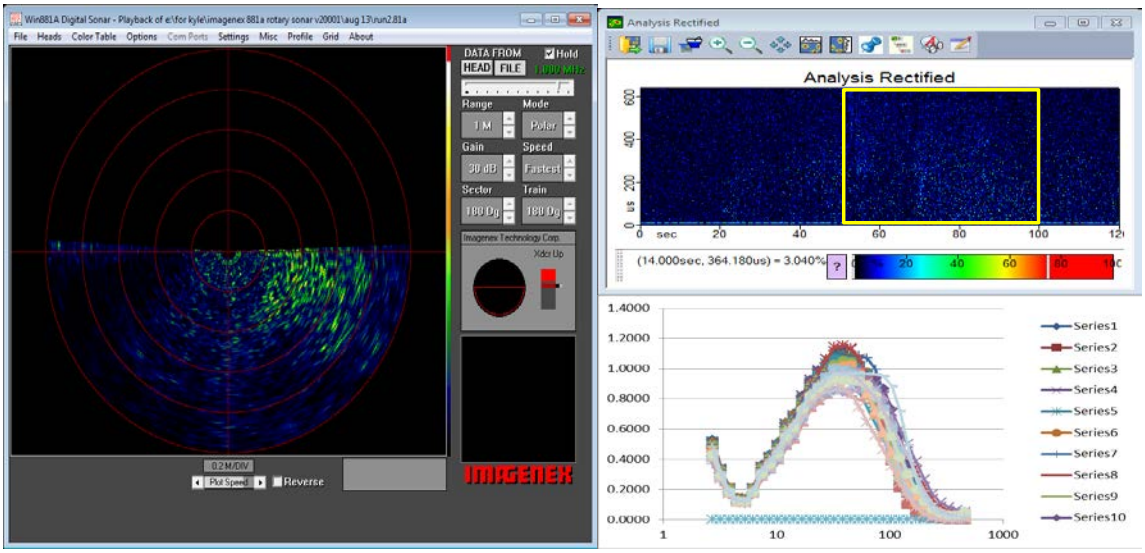

Figure 33. Imagenex sonar image at 1 MHz is at left for Run 2 from Ohmsett in August 2012. Our acoustic scattering at 1 MHz is also shown on the top right along with the droplet size distribution from the LISST at the bottom right.

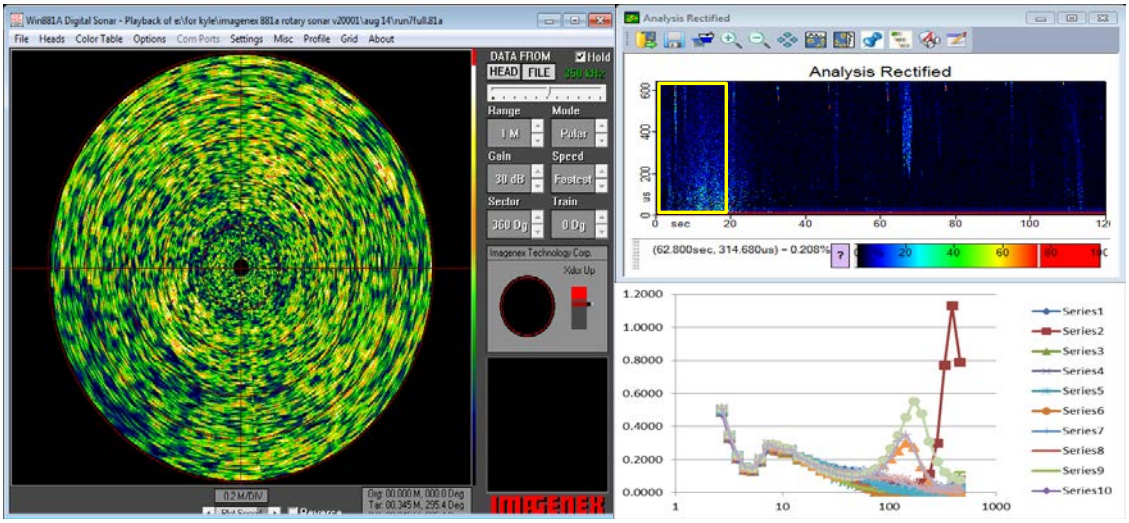

Figure 34. Imagenex sonar image at 350 kHz is on the left for Run 7 from Ohmsett in August 2012. Our acoustic scattering at 1 MHz is shown on the top right along with the droplet size distribution from the LISST at the bottom right.

These data show that the imaging sonar can detect particulates suspended in the water column and may be able to isolate specific sizes based on scattering over a larger frequency range. Sweeping the frequency to optimize scattering from different sized particulates would be a useful experiment, but was not in the scope of this project. This instrument is more promising for immediate deployment than the ADV because of the large frequency range and imaging capabilities. It would be beneficial if the vendor, Imagenex, stored the full acoustic waveform for custom processing.

3.6 SINTEF TOWER BASIN TESTING

We were able to participate in subsurface oil release experiments at the Sintef Tower Basin tank, which was not originally part of the scope of the project. The API is funding Sintef to perform various subsurface oil and dispersant release experiments. During one of these experiments we installed our instruments to measure the acoustic response of a subsurface oil plume. The measurements helped us to understand the differences between surface slicks and subsurface releases.

The Tower Basin is 3 meters across and 6 meters tall. Photographs of the tank and experimental setup are presented in Figure 35 through Figure 37. Figure 35 shows the acoustic instrumentation and cabling along with the pulser-receiver and laptop computer for data collection. The transducers were connected to a plastic holder shown in the right three photographs. We installed transducers with center frequencies of 0.5 MHz, 1 MHz, 2.25 MHz, and 5 MHz in the tank but only collected data with the 5 MHz transducer because of lack of time or opportunity for repetitive experiments. Figure 36 also shows the transducers installed in the Tower Basin placed directly opposite the Sintef LISST about 3 meters above the oil release. This height was chosen so that the LISST signal did not get saturated by high concentrations of oil.

The target oil flow rates were 0.5 L/min, 1.5 L/min and 3.0 L/min. Unfortunately it was difficult to maintain the proper flow rates and questions remain about the actual flow rates and droplet sizes achieved. For the configuration with the acoustic sensors directly across from the LISST, data were only collected at 1.5 L/min and 3 L/min. During testing the oil reservoir was depleted quicker than expected, further indicating problems with maintaining and measuring an accurate flow rate. While the reservoir was being refilled, we lowered the acoustic sensors below the LISST to about 1 meter above the release point to test the ability of the acoustics to image the entire width of the plume. This configuration is shown in the right hand photograph of Figure 37, prior to additional oil release. Figure 38 presents the acoustic data collected at both heights, with the left panel showing the data collected when the transducers were across from the LISST and the right panel data from below the LISST. The large color plot is the

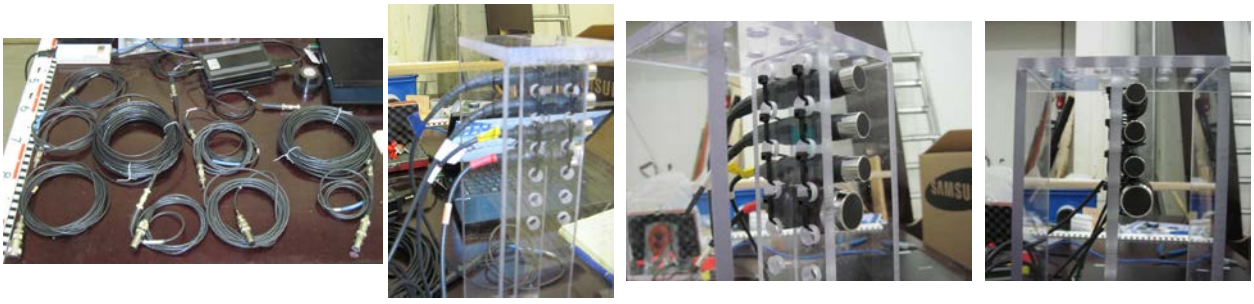

Figure 35 Photographs of the equipment setup at Sintef. The left panel shows the acoustic transducers lined up in order of frequency from left to right: 0.5 MHz, 1 MHz, 2.25 MHz and 5 MHz. The right three photographs show the transducers attached to the plastic holder for installation in the Sintef Tower Tank.

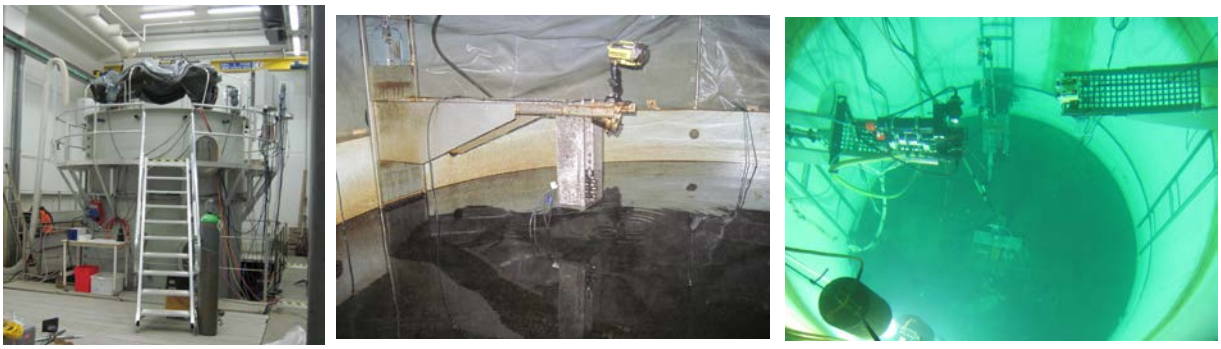

Figure 36 Photographs of the Sintef Tower tank and the installed acoustic sensors. The sensors were installed underneath the platform as shown in the center photograph. Video cameras were on top of the platform. The right photo show the sensors installed directly opposite the LISST.

acoustic backscattered signal as a function of propagation time along the horizontal axis with multiple pings stacked up along the vertical axis. The transducer was in clear water and sound propagated into and through the plume which can be seen as a vertical red region in the color plot in the right hand figure. The black plot along the top is the response from a single ping.

When the transducer was placed across from the LISST, it was on the edge of the plume and the scattering built up as the sound propagated into the plume then decreased in amplitude as it propagated through the plume. The horizontal distance along these plots is approximately 1 meter. For the scenario where the transducer was below the LISST the oil was pumped at 0.5 L/min, 1.5 L/min and 3 L/min then reduced to 1.5 L/min and mixed with Corexit 9500 at DOR of 1:50. Our preliminary measurements show the acoustic data scaled with changes in flow rate and thus droplet size for the position collected directly across from the LISST. We saw a 17% change in acoustic attenuation, in the direction expected, when the target flow rate increased from 1.5 L/min to 2 L/min. These flow rates were designed to produce 200 micron and 100 micron droplets, respectively. These sizes have not been confirmed with the LISST measurements yet because the API is waiting to release those data for publication. We

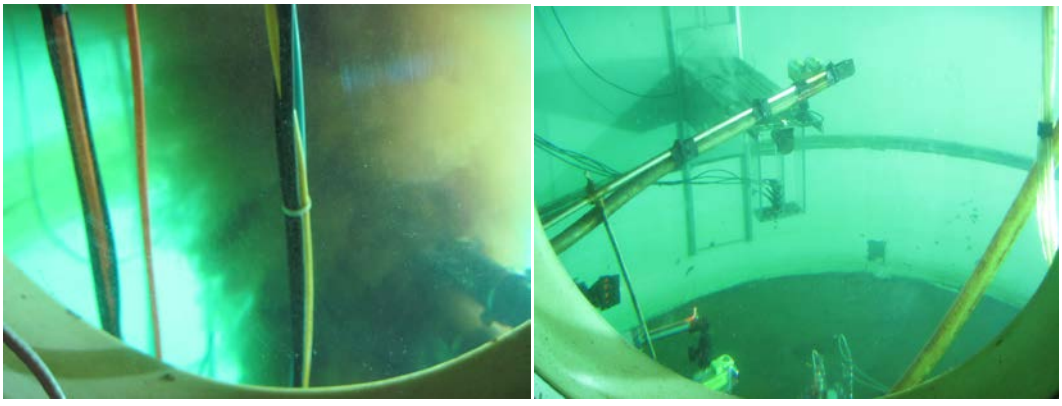

Figure 37. The left photograph shows the LISST encompassed by the plume as it rises. The right panel shows the acoustic sensors in the lower position, approximately 1 meter above the oil release.

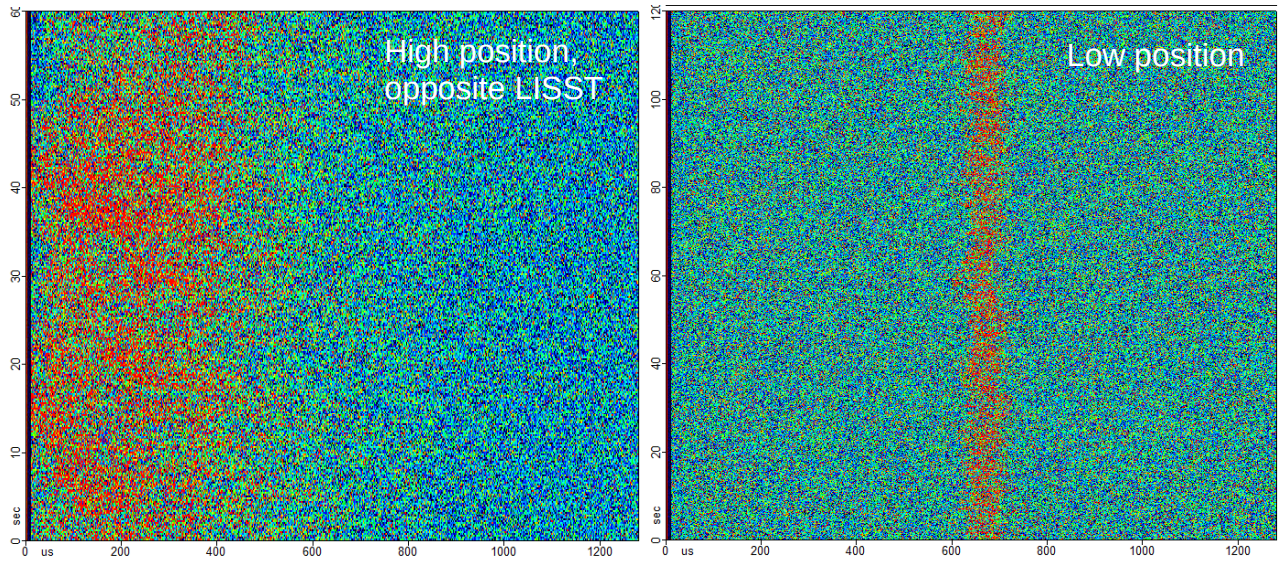

Figure 38. The acoustic backscattering signal at the high location is shown in the left hand panel and at the lower location in the right hand panel. The horizontal axis is the distance from the transducer and corresponds to 90 cm. The vertical axis is the ping or record number. The color represents the amplitude of the signal with red representing high scattering.

are having continued discussions with them so that we can benchmark these data. Below the LISST, the acoustics were able to penetrate the plume and image its width. While there were some subtle changes observed, there were no conclusive trends observed beyond measurement uncertainty. We are awaiting results from Sintef on their LISST measurements to draw further conclusions about our initial measurements in the Sintef Tower tank.

While the measurements at Sintef were not optimal because of the issues controlling the flow rate and the lack of repetitive measurements, it was important to collect data on a subsurface release of oil and dispersant to determine the similarities and differences between the surface releases we experienced at Ohmsett and in our laboratory and subsurface releases. In addition, during the testing at Ohmsett, the oil dispersion was not uniform in the pool, creating additional complications with analyzing and interpreting the data. While the Sintef tower tank is an excellent facility for creating subsurface plumes, the time during which measurements can be performed each week is limited to approximately 15 minutes, due to the immense size and logistics of filling and cleaning the tower tank. Even with these restrictions and challenges we are progressing in developing the relationships between oil droplet size and acoustic properties. Our data have shown subsurface releases of oil and applications of dispersants create different measurement challenges relative to surface slicks and above water dispersant applications where the concentrations and flow rates are relatively low. It is clear that additional testing on better-controlled subsurface releases, including smaller scale laboratory experiments, is needed to continue development and refinement the acoustic measurements.

3.7 MIXTURES OF OIL, DISPERSANT, AND AIR

During our laboratory testing, we inadvertently injected a significant amount of air into the oil-water and oil-water-dispersant mixtures causing several experimental data sets to be unusable for determining oil droplet size. While not ideal for this project, in retrospect, these measurements were useful for the overall goal of characterizing oil plumes because gas bubbles are expected to be present in a blowout. In fact, during the Deepwater Horizon incident it was estimated that the plume consisted of approximately 22% natural gas [Camilli]. Advancements in measurement technologies are needed to separate the responses from oil droplets and natural gas bubbles in a plume so that the oil droplet size can be accurately measured to determine the dispersant efficacy.

Our preliminary results with bubbles in the water column are shown in Figure 39 and Figure 40 using the small sample chamber. Figure 39 shows acoustic images for gently mixed water with very few bubbles and vigorously mixed water with many air bubbles for 2 minutes. The droplet size distribution from the LISST is shown in the right panel for the vigorously mixed water showing a bimodal distribution with peaks near 20 microns and 100 microns. The air bubbles strongly scatter the acoustic waves and individual bubbles can be seen to move through the acoustic field as they rise to the surface; most of the bubbles are out of the acoustic field in 60 seconds.

The acoustic response from an oil-gas-water mixture is shown in. This mixture caused the acoustic wave to scatter, creating a bright orange/red pattern between zero

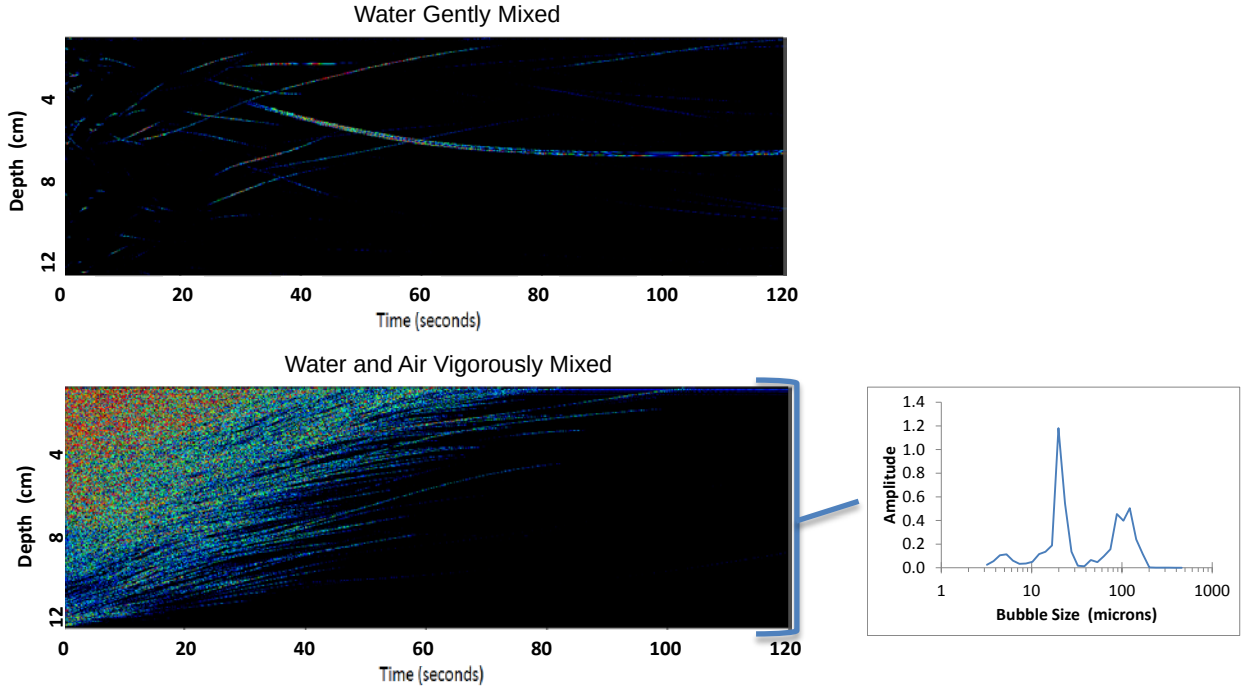

Figure 39 Acoustic scattering images of gently mixed water with very few gas bubbles (top left) and vigorously mixed water with many air bubbles (bottom left). The bubble size distribution from the LISST measurements is shown at right.

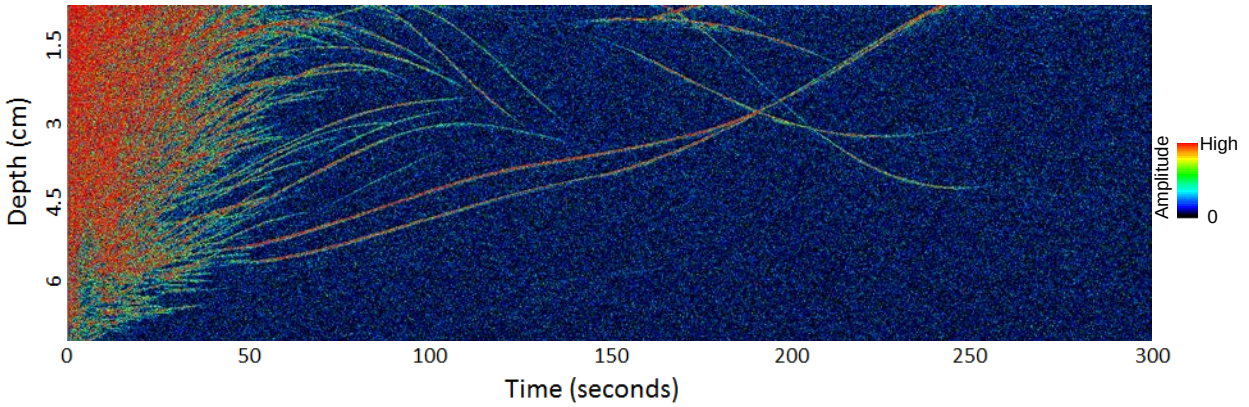

Figure 40. Acoustic images of the scattering from a Canadian Hebron oil-air mixture in water over 300 seconds. An individual ping is shown on the right hand side of each figure. The red/orange regions are high scattering and the black/dark blue is low scattering. The long tracks are individual particulates (drops or bubbles) as they move through the field of view of the 5 MHz transducer.

and ~30 seconds. After ~ 30 seconds, scattering from the bubbles and/or oil droplets caused distinguishable orange/red streaks. The streaks generally pointed up with some streaks pointing left to right or down - presumably from random motion in the chamber. The droplets and bubbles continued to move through the field of view of the transducer for up to ~ 250 seconds. The backscattered acoustic signal ~10 seconds after the transducer was inserted is shown at the right of the image. The particulate size distribution from the LISST shown in Figure 41 is also bimodal (like the bubble-water mixture), but with a higher number of larger particulates.

At this time these measurements do not allow us to distinguish the oil droplets from gas bubbles, but provide information about the qualitative dynamics of the bubble-oil mixtures and their size distributions of the mixtures. This information is useful in that it shows that we can expect strong scattering from air bubbles, and that they rise out of the field of view quickly. It also shows that the mixture of gas and oil is very buoyant and rises to the surface faster than the oil only mixtures shown in previous figures.

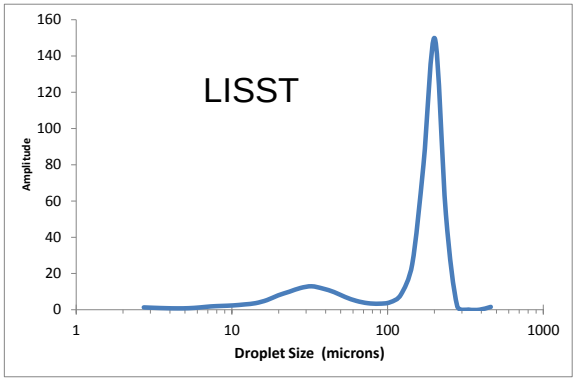

Figure 41 The size distribution of the oil-gas-water mixture from the LISST. Similar to the air-water system the distribution is bimodal, but with a larger number of larger scatterers.

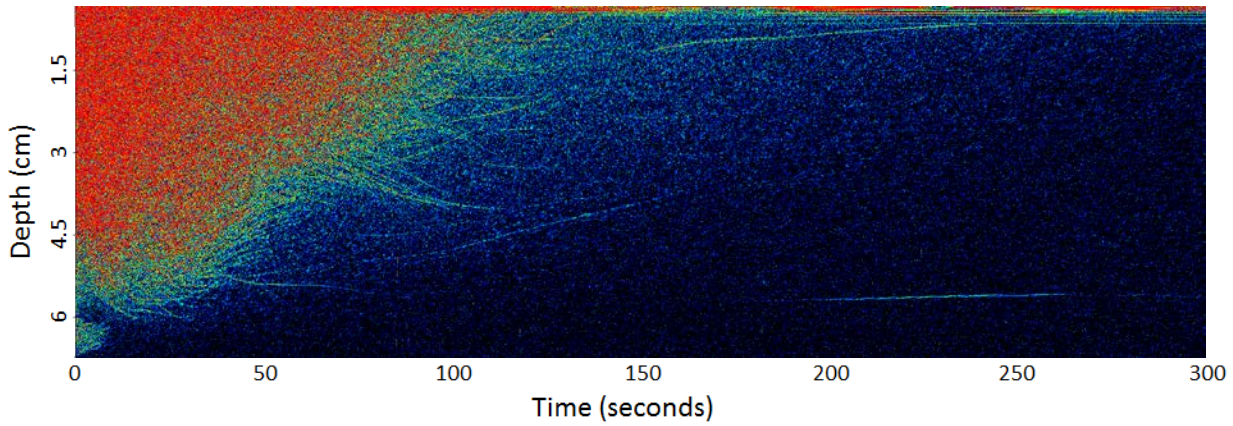

Figure 42 Acoustic measurements on Canadian Hebron oil and Corexit 9500 at a DOR of 1:4 with vigorous mixing which entrained air bubbles with the oil-dispersant mixture.

We also added Corexit 9500 to the Canadian Hebron oil at a DOR of 1:4 to see if the dispersant would help overcome the added buoyancy of the air bubbles. The resultant scattering is shown in Figure 42 over a 5 minute period. The dispersant did indeed keep the oil suspended below the water surface for a longer period of time with the high scattering indicated in orange and red extending out nearly 2 minutes. Interestingly the tracks at later times appeared smaller than the tracks in Figure 40. No attempt was made to determine what portion of the scattering was attributed to dispersed oil, undispersed oil or air bubbles. Our future work will focus on determining these relationships for subsurface releases of oil-bubbles and dispersant mixtures.

3.8 MIXTURES OF OIL AND SEDIMENT

When a blowout from the seafloor occurs, it is possible for sediment to get entrained in the plume. Therefore it is important to determine what effects sediment produces on oil dispersability. Sediment may also become entrained in an oil spill if it occurs in a sediment laden river or impinges on a shoreline. We performed initial acoustic measurements on suspended sediment by first measuring sand and mud separately in the small chamber with the transducer pointed down. Images of the acoustic response are shown in Figure 43. The orange region in the first 15 seconds of the top panel is the scattering from the sand as it rapidly settled to the bottom of the chamber. A few individual tracks of particles moving up and down after approximately one minute is likely due to turbulence and the presence of finer particles. We then added mud to the sand and mixed it vigorously by drawing the sediment-water mixture into a 60 mL syringe as we did with previous experiments with oil. The sand settled out very quickly, but the mud remained suspended for several minutes with multiple particulates moving through the field of view of the transducer for over 300 seconds. Some of the finer mud particles, which can have diameters under 10 microns, were suspended for several minutes. During mixing we may have introduced air bubbles which could also account for the upward moving tracks observed early in the run.

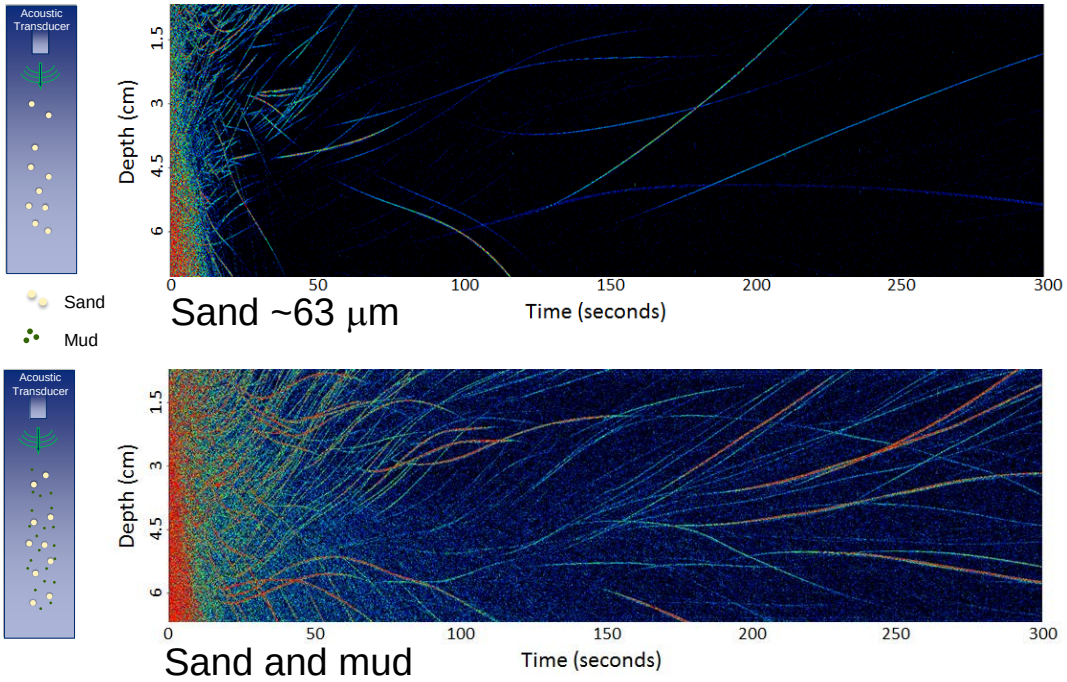

Figure 43. Acoustic scattering from sand and sand-mud mixtures showing the sand settling rapidly while the mud remaining suspended for longer periods of time.

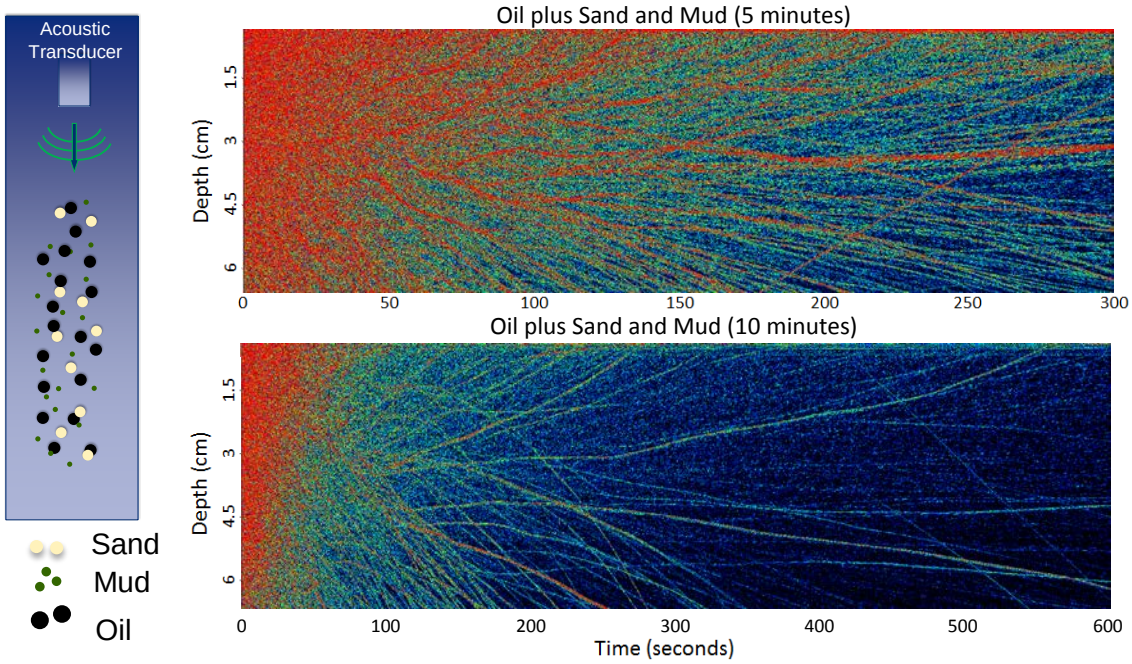

Figure 44. A mixture of Canadian Hebron oil and sediment (sand and mud) shows the sediment significantly increased the dispersability of the oil.

After performing measurements on the sand-mud mixture, we added a small amount of Canadian Hebron oil and mixed it vigorously with the 60 mL syringe. The resultant acoustic backscattering is shown in Figure 44 over 5 minutes in the top panel and 10 minutes in the bottom panel. The sediment clearly enhanced the dispersability of the oil and kept it in suspension well beyond 2 minutes, in contrast to the oil mixtures in Figure 40 and Figure 42. Again, we may have inadvertently inserted air into the mixture, causing the oil to rise more rapidly. However, even if air was injected, the oil was suspended for several minutes. At this point it is not possible to determine which tracks are associated with oil and which are from the sand, mud or air. It would be valuable to study the interactions of oil, air, and sediment in water columns in future projects.

4. SUMMARY AND CONCLUSIONS

Our goal in this project was to begin development of practical tools to measure oil droplet size in-situ using acoustic scattering methods. We conducted measurements in our laboratory, at Ohmsett over 6 days (one day in December 2011 and five days in August 2012) and at the Sintef Tower Basin on a subsurface release. In total, we made measurements on 6 different oils and 2 different dispersants. From the data collected during these tests, we developed methods to measure dispersed oil droplet size using acoustic attenuation at 5 MHz. This frequency was well above the resonant frequency of the oil droplets and thus made the interpretation relatively straightforward.

Our testing has shown subsurface releases of oil and application of dispersants creates different measurement challenges relative to above water dispersant applications to surface slicks. More specifically, the oil concentration is higher in the plume, the oil is more localized in the plume rather than spread out, and the droplet speeds are dramatically different between surface slicks (low speed) and subsurface blowouts (high speed). We also measured the changes in dispersability using acoustic scattering methods with mixtures of oil, dispersant, and air bubbles, and oil and sediment. The sediment increased the dispersability of Canadian Hebron oil by about a factor of 3, while air bubbles decreased the dispersability. Adding Corexit 9500 at a DOR of 1:4 overcame some of the decrease in dispersability due to air bubbles (by about a factor of 2).

As part of this project we assessed an Imagenex imaging sonar system which operates between 340 kHz and 1 MHz and a Sontek ADV for near-term application to measuring oil dispersions and future technology transfer. We determined that the imaging sonar can indicate that particulates are suspended in the water column and may be able to isolate specific sizes based on scattering over a larger frequency range. The ADV could also identify that particulates were in the water column, but also could not be used to measure droplet size in its current configuration.

Overall, the results are very encouraging and are a significant step in the development of in-situ field methods for measuring oil droplet size using acoustic scattering.

5. RECOMMENDATIONS AND FUTURE WORK

There is a long list of parameters that the oil spill response community desires to measure to help optimize the application of dispersant to subsea blowouts. Parameters of interest include the size distribution of the oil droplets, the presence and size distribution of gas hydrates and gas bubbles, the presence and size distribution of any sediment, and the dynamics of these constituents as a function of depth, temperature, salinity, and dispersant-to-oil ratio (DOR) [Ahnell, Nedwed]. Studying the dynamic interactions of these constituents is recommended to help guide the development of practical tools to measure dispersant effectiveness.

In this project we first showed the proof-of-concept for acoustic scattering to measure oil droplet size well above the resonant frequencies. We focused on surface slicks and laboratory measurements so that multiple measurements could be performed quickly. Now that we have demonstrated the proof-of-concept and performed initial measurements on subsurface releases at Sintef, we recommend additional experiments with better-controlled subsurface releases to develop the acoustic measurements for the relevant subsea plume conditions.

Further measurements are needed to refine and validate the oil droplet size calibration curve we developed at 5 MHz and to compare our measurement over a larger frequency range with theoretical predictions. We recommend additional work on a broader range of oils over a wide range of viscosities. As noted below, future work should include the addition of gas bubbles and sediment.

It will also be important in the future to determine the three dimensional properties of the dispersed oil and plumes. In addition, we recommend putting these acoustic measurements on ROVs and AUVs so that the full acoustic waveforms can be collected and analyzed rather than the subset available in commercial instruments.

Finally, we recommend a “two-pronged” approach for future development; one path should focus on instrument development and a second path on scientific studies. The goal of the first path will be to develop acoustic instruments at specific frequencies to optimally excite droplets so that the instruments can measure the transition from large droplets that will rise to the surface to small droplets that will stay entrained in the water column after a dispersant application. The goal of the second path will be to continue the scientific study of multi-particulate plumes to develop methods to accurately measure key parameters in-situ (discussed above) to help optimize the application of dispersant to subsea blowout oil.

6. REFERENCES

Arden Ahnell, Personal communication, 2012

Agrawal, Y.C. and Pottsmith H.C., 2000. Instruments for particle size and settling velocity observations in sediment transport. Marine Geology, 168, 89-114.

Belore RC, Trudel K, Mullin JV, Guarino A (2009): Large-scale cold water dispersant effectiveness experiments with Alaskan crude oils and Corexit 9500 and 9527 dispersants. Marine Pollution Bulletin 58:118-128

Camilli et al. "Acoustic measurement of the Deepwater Horizon Macondo well flow rate" PNAS, 2011

Cartwright, G.M., C.T. Friedrichs, and P.D. Panetta, 2012. Dual use of a sediment mixing tank for calibrating acoustic backscatter and direct Doppler measurement of settling velocity. OCEANS 2012, Institute of Electrical and Electronics Engineers, CD ISBN 978-1-4673-0830, 7

Imagenex, 2004, Imagenex Moxel 881 Digital Multi-Frequency Imaging Sonar Manual, www.imagenex.com.

Alun Lewis and D. Aurand, Putting Dispersants to Work. Overcoming Obstacles, API Publ. 4652A, American Petroleum Institute, Washington, D.C. (1997)

Lohrmann, A., 2001. Monitoring sediment concentration with acoustic backscattering instruments. Nortek Technical note no 3. www.nortek-as.com. 5 p.

Medwin, H. (2005) Sounds in the Sea: From Ocean Acoustics to Acoustical Oceanography. Cambridge University Press.

Nortek, 2005. Vector current meter user manual. Doc No N300-100. www.nortek-as.com.

National Commission on the BP Deepwater Horizon Oil Spill and Offshore Drilling, "Deepwater The Gulf Oil Disaster and the Future of Offshore Drilling", Report to the President, 2011.

National Commission on the BP Deepwater Horizon Oil Spill and Offshore Drilling, "The Use of Surface and Subsea Dispersants During the BP Deepwater Horizon Oil Spill", Staff Working Paper No. 4, Draft, 2010

Tim Nedwed, Personal Communication, 2012

Paul D. Panetta, Leslie Bland, Grace Cartwright, and Carl T. Friedrichs, "Acoustic scattering to measure dispersed oil droplet size and sediment particle size", Proceedings of the Oceans 12 Conference 2012.

P. D. Panetta, B. J. Tucker, R. A. Pappas, and S. Ahmed, “Characterization of Solid Liquid Suspensions Utilizing Ultrasonic Measurements,” Rev. of Prog. in QNDE, 22B, 2002.

P. D. Panetta, B. J. Tucker, R. A. Pappas, and S. Ahmed, “Characterization of Solid Liquid Suspensions Utilizing Ultrasonic Measurements,” IEEE Meas Science and Tech, 2003.

Paul D. Panetta, “Ultrasonic Characterization of Solid-Liquid Suspension” US Patent 7,739,911, 2010

Traykovski, P., Latter, R.J., and Irish, J.D., 1999. A laboratory evaluation of the laser in situ scattering and transmissometry instrument using natural sediments. Marine Geology 159: 355-367.

Robert J. Urick, “Principles of underwater sound”, 3e, Mc Graw Hill 1983

Sontek, 2001. Getting started with the ADVField/Hydra system. San Diego, CA. www.sontek.com.

Sontek, 2013. ADVOcean brochure, http://www.sontek.com/pdf/brochures/advocean-web-reduce.pdf, downloaded 1/16/2013.